SARS-CoV-2 transmission across age groups in France and implications for control

Cécile Tran Kiem, Paolo Bosetti, Juliette Paireau, Pascal Crepey, Henrik Salje, Noémie Lefrancq, Arnaud Fontanet, Daniel Benamouzig, Pierre-Yves Boëlle, Jean-Claude Desenclos, et al.

Title: SARS-CoV-2 transmission across age groups in France and implications for control

Authors:

Cécile Tran Kiem[1,2], Paolo Bosetti[1], Juliette Paireau[1,3], Pascal Crépey[4], Henrik Salje[1,5], Noémie Lefrancq[1,5], Arnaud Fontanet[6,7], Daniel Benamouzig[8], Pierre-Yves Boëlle[9], Jean-Claude Desenclos[3], Lulla Opatowski[10,11], Simon Cauchemez[1,*]

Affiliations:

1. Mathematical Modelling of Infectious Diseases Unit, Institut Pasteur, UMR2000, CNRS, Paris, France
2. Collège Doctoral, Sorbonne Université, Paris, France
3. Santé publique France, French National Public Health Agency, Saint-Maurice, France
4. Univ Rennes, EHESP, REPERES « Recherche en Pharmaco-Epidémiologie et Recours aux Soins » – EA 7449, Rennes, France
5. Department of Genetics, University of Cambridge, Cambridge, UK
6. Emerging Diseases Epidemiology Unit, Institut Pasteur, Paris, France
7. PACRI Unit, Conservatoire National des Arts et Métiers, Paris, France
8. Sciences Po - Centre de sociologie des organisations and Chaire santé - CNRS, Paris, France
9. Sorbonne Université, INSERM, Institut Pierre Louis d'Epidémiologie et de Santé Publique, Paris, France
10. Institut Pasteur, Epidemiology and Modelling of Antibiotic Evasion (EMAE), Paris, France
11. Université Paris-Saclay, UVSQ, Inserm, CESP, Anti-infective evasion and pharmacoepidemiology team, Montigny-Le-Bretonneux, France

*** Corresponding author:** Simon Cauchemez, Mathematical Modelling of Infectious Diseases Unit, Institut Pasteur, 28 rue du Dr Roux, 75015, Paris, France, simon.cauchemez@pasteur.fr

Abstract

The shielding of older individuals has been proposed to limit COVID-19 hospitalizations while relaxing general social distancing in the absence of vaccines. Evaluating such approaches requires a deep understanding of transmission dynamics across ages. Here, we use detailed age-specific case and hospitalization data to model the rebound in the French epidemic in summer 2020, characterize age-specific transmission dynamics and critically evaluate different age-targeted intervention measures in the absence of vaccines. We find that while the rebound started in young adults, it reached individuals aged ≥80 y.o. after 4 weeks, despite substantial contact reductions, indicating substantial transmission flows across ages. We derive from these patterns the contribution of each age group to transmission. While shielding older individuals reduces mortality, it is insufficient to allow major relaxations of social distancing. When the epidemic remains manageable (R close to 1), targeting those that contribute more to transmission is better than shielding at-risk individuals. Pandemic control requires an effort from all age groups.

To mitigate the impact of COVID-19 during the first year of the pandemic, many countries implemented drastic social distancing measures that proved effective at reducing the stress on the healthcare system [1,2] but were associated with major social and economic costs because they required an effort from all. Since infections leading to hospitalization and death were concentrated in elderly people and people with comorbidities, some argued that strategies that shield at-risk individuals from infection (for example by isolating them) could be used to maintain hospitalizations at low levels while relaxing costly social distancing measures that affect the rest of society [3,4], which has raised substantial debates [5–7]. These arguments resonate with decades-old debates on the relative contribution to disease control of strategies that target at-risk individuals versus disease transmitters [8–13].

The massive roll-out of safe and effective vaccines [14–16] should ensure that countries no longer need to resort to drastic social distancing measures such as lockdowns to control COVID-19 epidemics. Nonetheless, it remains important to determine whether, in the absence of vaccines, strategies shielding at-risk individuals may allow the relaxation of social distancing measures since i) COVID-19 vaccine coverage remains low in many countries and ii) shielding strategies may be considered at the start of future emergences when no vaccines are available yet. Such evaluation requires a detailed understanding of the dynamics of transmission of SARS-CoV-2 across age groups. We perform such assessment by analysing the epidemic rebound that occurred in France in the summer-autumn 2020. In France, the nationwide lockdown implemented in spring 2020 [1] was followed by the progressive relaxation of social distancing measures, the scaling up of a strategy based on testing, contact tracing and case isolation and the general use of face masks. However, this did not impede a large second wave in the autumn and a new lockdown in November 2020.

Here, we build a modeling framework to reconstruct the complex patterns of spread of SARS-CoV-2 across age groups along with the dynamics of infections and hospitalizations, from the detailed analysis of age-stratified case (N=368,906) and hospitalization (N=16,548) data from all 13 regions of Metropolitan France, between 15 June and 28 September 2020. We fit our model to age-stratified hospital admissions and positivity rates among symptomatic individuals that received a RT-PCR test result (labelled symptomatic individuals in the rest of the text). Based on these dynamics, it is possible to quantify the contribution of each age group to transmission. This characterization can then be used to critically evaluate different age-targeted intervention measures implemented in the absence of vaccines. We only consider interventions targeting members of the general population (i.e. we do not assess measures targeting specific settings such as elderly homes, hospitals or prisons). We first detail the results for Auvergne-Rhône-Alpes (8 million inhabitants), which was one of the first regions to experience an epidemic rebound (Figure S1); and then present results for all 13 regions in metropolitan France.

Results

Epidemic dynamics across age-groups

In the Auvergne-Rhône-Alpes region, the proportion of positive tests among symptomatic individuals aged 20-29 y.o. increased from 3.2% to 12.9% between 27 July 2020 and 17 August 2020 (Figure 1A). This increase was quickly followed by a rise in positivity rates (Figure 1A, 1B)

and hospital admissions in other age groups (Figure 1C, 1D). For example, in the week of 14 September 2020, 10.8% of symptomatic individuals aged ≥80 y.o. were positive (compared to 0.7% on the week of 17 August 2020) and there were 169 hospital admissions of patients in that age group (compared to 23 on the week of 17 August 2020). These trends were observed across all metropolitan French regions, with a mean lag of 4 weeks between the increase in the proportion of positive tests among symptomatic individuals aged 20-29 y.o. and those older than 80 y.o. (Figure 1E). This indicates substantial porosity of transmission between age groups.

Estimates of the contribution of different age groups to transmission

To quantify the impact of interventions over time, it is important to note that effective reproduction numbers naturally decline as the proportion of susceptible individuals declines, even if transmission rates remain the same. Here, we introduce the intervention reproduction number Ri as the average number of infections resulting from a single index case under a set of interventions if the population was completely susceptible. Fitting our model to these data, we estimate that, in Auvergne-Rhône-Alpes, R_i increased from 0.71 (95% credible interval: 0.69-0.73) during the lockdown to 0.90 (95% CrI: 0.88-0.93) between 11 May and 8 July and to 1.46 (95% CrI: 1.44-1.49) from 9 July to 28 September 2020 (Figure 2A, Table S1).

We define daily effective contacts as model predicted daily contacts in the estimated mixing matrix rescaled so that the number of daily effective contacts in the 20-29 years old is 7.7, as observed in the SocialCov survey (Figure S2). We estimate that the number of effective contacts in the rebound period starting on 9 July was highest in individuals aged 20-29 y.o (Figure 2B, Figure S2-S3). As a comparison, the number of effective contacts in those aged 10-19 y.o., 50-59 y.o. and ≥80 y.o. was respectively 5.9 (5.3-6.5), 4.5 (3.9-5.2) and 2.9 (2.4-3.4), corresponding to 0.76 (0.69-0.84), 0.59 (0.51-0.68) and 0.38 (0.31-0.45) times the number of effective contacts in individuals aged 20-29 y.o. These estimates are consistent with the number of daily contacts measured in different age groups by the online survey SocialCov (30 July-27 September 2020) (see Supplementary Information) [17], but for two key differences (Figure 2B). First, we estimated that the number of effective contacts for transmission in children aged 0-9 y.o. was substantially lower than the reported number of contacts in the survey. This reflects the limited contribution of younger children (0-9 y.o.) to SARS-CoV-2 transmission during this time period and is consistent with either a lower susceptibility to SARS-CoV-2 infection or a reduced infectivity compared to older individuals [18–21]. Second, the contribution to transmission of all other age groups relative to those aged 20-29 y.o. is between 17% and 37% lower than what might be expected from the contact survey. Again, this might be explained by reduced risks of transmission given contact compared to 20-29 y.o., for example thanks to better compliance with the use of masks or physical distancing. These differences highlight the distinction between raw contacts measured from contact surveys and effective contacts that we estimate and that capture different risks of transmission given contact. Our estimated mixing patterns can reproduce the observed rises in positivity rates (Figure 2C,E, Figure S4, Figure S5) and hospital admissions by age group (Figure 2D,F, Figure S4, Figure S6).

Impact of strategies shielding the elderly population in the absence of vaccines

We use our model to assess the potential impact of social distancing measures targeting different age groups in the absence of vaccines. We further assume that when individuals reduce their contacts, their contacts are affected homogeneously irrespective of their age.

In Auvergne-Rhône-Alpes, the effective reproduction number R_{eff} (i.e. the average number of infectious individuals infected by an index case accounting for the build-up of immunity) increased from 1.3 to 1.5 during the build-up of the Autumn wave [22–24]. Even though this corresponds to a 50% reduction in the transmission rate compared to a scenario with no control measures [1], this was insufficient to avoid a surge in hospitalizations and eventually the implementation of a national lockdown on 30 October 2020. We explore whether shielding individuals aged ≥70 y.o. could have been sufficient to maintain the epidemic at manageable levels for hospitalizations while relaxing control measures so that the effective reproduction number would be R_{eff}≥1.3-1.5. We deliberately consider an "extreme" scenario of shielding where the number of effective contacts of the target age group would be reduced by 50% to be similar to what was measured during the lockdown of March-May 2020 [17]. Going further than this reduction seems difficult as this lockdown was already very strict. We find that in the range R_{eff} = 1.3-1.5, this would still result in 53-116 per million daily hospital admissions at the peak, above the national peak of March-April 2020 (56 per million) (Figure 3A) and 664-1074 deaths per million (Figure 3B). Further relaxing control measures up to R_{eff}=1.8 would increase the peak daily number of hospitalized patients to 233 per million and the overall number of deaths to 1646 per million. Applying these reductions to individuals ≥60 y.o. would not avoid a surge of COVID-19 patients in hospitals, shall control measures be relaxed (Figure S7).

Impact of strategies targeted towards different age groups

This suggests that shielding elderly individuals would not allow an important relaxation of social distancing measures as the effective reproduction number needs to be maintained close to 1 for the epidemic to remain manageable. This requires efforts from all age groups. In this latter context of a slowly growing epidemic characterized by R_{eff} close to 1, we investigate if it would be better from a public health perspective to reduce contacts of elderly individuals rather than those of other age groups. We find that, for R_{eff} close to 1, targeting 20-29 y.o. individuals, i.e. the age-group with the largest number of effective contacts, results in the largest reduction in key epidemiological metrics. For example, considering the example of the region Auvergne-Rhône-Alpes, in a scenario where $R_{eff} = 1.1$, the peaks in new infections (Figure 4A), hospital admissions (Figure 4B) and ICU admissions (Figure 4C) and the number of deaths (Figure 4D) would all drop by 33%, if all individuals aged 20-29 y.o. reduced their average number of effective contacts by 1 (i.e. from 7.7 contacts per day to 6.7 on average), compared to 6%, 16%, 11% and 26%, respectively, if those aged ≥80 y.o. were targeted instead (from 2.9 to 1.9 contacts per day on average).

We found in the previous section that the healthcare system would be unable to cope with large values of the reproduction number even if elderly individuals were shielded. We nevertheless

explore such scenarios in case the cost of control measures was judged too elevated by decision makers. As the reproduction number increases, the same efforts in terms of reductions of contacts would lead to lower impact on key epidemiological metrics; and the ordering of strategies may change towards a higher efficiency of strategies targeting those most at risk of severe outcomes. Targeting ≥80 y.o. individuals becomes the best strategy to reduce deaths when R_{eff} is ≥1.17 (Figure 4D). For instance, if $R_{eff} = 1.6$, the number of deaths would drop by 22% if we removed 1 effective contact for those 80 y.o. and older; but by only 6% if we targeted those aged 20-29 y.o. We find a similar pattern if the objective is to minimize the number of life-years lost and quality-adjusted life years (Figure S8). For large values of R_{eff}, we obtain relatively similar reductions on peak hospital admissions irrespective of the target group among all age groups ≥20 y.o. To reduce peak ICU admission, it remains slightly less interesting to target those aged ≥80 y.o. since this population is less likely to be admitted in ICU. The largest reduction in the peak number of infections is always obtained targeting groups significantly contributing to transmission irrespective of the value of R_{eff}. These conclusions remain unchanged when a larger number of effective contacts is being removed, although the impact on epidemiological metrics increases (Figure S9-S10).

As the number of effective contacts differs between age groups (Figure 2B), a reduction of 1 effective contact does not correspond to the same effort in the different age groups. For example, removing 1 effective contact per day corresponds to a 13% reduction of contacts in individuals aged 20-29 y.o., but a 35% reduction in those aged ≥80 y.o. Applying the same 20% reduction of effective contacts in all age groups, we find that the largest reduction in the peak of new infections, hospital admissions and ICU admissions is obtained when targeting the 20-29 y.o. regardless of the effective reproduction number value (Figure S11). The optimal strategy to minimize the number of deaths targets those aged ≥80 y.o. when R_{eff}≥1.46 (compared to ≥1.17 for an absolute reduction of 1 contact) (Figure S12). To account for the fact that different age groups have different numbers of contacts and different capacities to reduce contacts, we can also compare strategies where the same number of individuals are put into lockdown in the different age groups (Figure S13). In this scenario, we also find that optimal strategies shift from targeting those that contribute the most to transmission for R_{eff} <1.3 (Figure 5) to targeting older individuals for larger values of R_{eff}.

Results across regions in metropolitan France

Our model can reproduce the dynamics of test positivity in symptomatic individuals and hospitalizations across all the regions of metropolitan France (Figure S14-S25). We also find consistent patterns regarding the numbers of effective contacts by age group across regions(Figure S26), with the highest values observed in individuals aged 20-29 y.o. In 10 out of 12 regions of Metropolitan France, we reach similar conclusions that in situations characterized by R_{eff} close to 1 where the epidemic may remain manageable, it is beneficial to reduce effective contacts of those that contribute the most to transmission; while for larger values of R_{eff} that are likely to lead to a major crisis in hospitals, it is optimal to target those with the highest risk of severe outcome (Figure 4E-H, Figure S8). The two regions where we find it is beneficial to start

targeting older individuals to maximize the reduction in deaths when R_{eff} is low are characterized by low estimates of the number of contacts in those aged ≥80 y.o. (respectively 1.55 (1.03-2.18) for Nouvelle-Aquitaine and 2.38 (1.77-3.09) for Provence-Alpes-Côte d'Azur) and are the metropolitan French regions with the highest proportion of ≥80 y.o. in their population.

Sensitivity analyses

In a sensitivity analysis, we vary assumptions about the relative infectivity and susceptibility of the different age groups and the way we model the impact of interventions targeting different age groups. We find consistent results regarding the contribution of age groups to transmission (Figure 6A, Figure S27). In all scenarios, individuals aged 20-29 y.o. contribute the most to transmission, children aged 0-9 y.o. have a limited contribution (between 0.14 and 0.31 times the contribution of the 20-29 y.o. across scenarios) and among those aged 20 y.o. and older, the contribution of the different age groups decreases with age. Across these scenarios, the magnitude of the contribution to transmission of the 10-19 y.o. is roughly similar to that of the 30-49 y.o. We find higher heterogeneity between age groups when assuming that contacts are only modified outside the household and a lower heterogeneity when considering quadratic reductions in contact patterns. Interestingly, we find similar estimates when varying assumptions regarding the infectivity and susceptibility of the different age groups, which suggests that the notion of effective contacts captures the actual contribution of the different age groups to transmission, including their varying infectivity or susceptibility. Across these scenarios, we explore the correlation between the number of contacts reported in the SocialCov contact survey and the number of contacts estimated, by adjusting our estimated effective contacts for changing assumptions regarding the infectivity and susceptibility of the different age groups. Accounting for a reduced susceptibility in those aged 0-19 y.o. provides the highest correlation (Figure S28). Exploring the impact of strategies targeting specific age groups across these sensitivity analyses, we find that the shielding of older individuals is insufficient to avoid an important surge in hospitalizations and deaths (Figure 6B,C) and that the most efficient strategy to minimize deaths shifts from targeting those that contribute most to transmission to those most at risk of severe outcomes as R_{eff} increases (Figure 6D).

Discussion

At the start of the COVID-19 Autumn wave in 2020, we observed a very consistent epidemiological pattern across the 13 regions of metropolitan France. It started with an increase of infections among young adults, that was followed up by a rise in infections in other age groups and eventually in older individuals. Similar patterns have been described in other locations [25–27]. This indicates substantial porosity of transmission across age groups. We used our model to quantify this phenomenon and evaluate non-pharmaceutical control strategies targeting different age groups. We found that even if we managed to reduce effective contacts of older individuals by 50%, this would not allow important relaxations of control measures in the absence of vaccines. In practice, it is unclear whether it would be possible to achieve such reductions for this age group since i) older individuals already behave very carefully with a number of effective contacts that is

2 to 5 times lower than that of those aged 20-29 y.o and ii) they are often dependent persons with a minimum number of contacts required for their basic daily activities. In all instances, our results indicate that to avoid a major crisis in hospitals, in the absence of vaccines, it is essential to maintain transmission rates at relatively low levels (with R_{eff} close to 1) which requires an effort from all. For this parameter regime where R_{eff} is close to 1, reducing contacts in younger age groups who contribute more to transmission would have a larger impact on key epidemiological indicators than targeting at-risk individuals.

Besides, strategies based on shielding a single part of the population, like the elderly, may raise serious ethical and social concerns. Such strategies can easily fuel societal controversies undermining social cohesion ("age-itation"), often viewed as a key asset in the management of the epidemic [28,29]. Differentiated strategies might also modify the compliance of certain groups to other measures, which could reduce their impact. From a broader social perspective, the focus on the elderly would also represent a breach in values of solidarity between citizens and generations, which is considered as a cement of the welfare state in countries like France. The isolation of the elderly would erode social ties and weaken their situation, with strong concerns on ethical principles such as autonomy and benevolence [30]. From a wider political perspective, such strategies would also represent a shift in the legitimacy of the State to intervene to control the epidemic: by promoting self-protection strategies rather than collective measures, governments will weaken their own capacity to intervene, leaving ground to more individualistic strategies.

We critically evaluated measures targeting members of the general population of different age groups without assessing measures targeting specific settings such as elderly homes, hospitals or prisons, where transmission dynamics are expected to be different[31]. In France, like in a number of other countries, elderly home residents were strongly impacted by the pandemic, representing more than 40% of deaths until February 2021. Shielding elderly home residents was therefore rightly considered a priority to mitigate pandemic impact. Here, we investigated whether, in addition to epidemic control in elderly homes, shielding of individuals aged 70 y.o. and older that do not live in elderly homes (about 93% of the age group[32]) might allow important relaxation of control measures in the absence of vaccines. This was done by excluding elderly home residents from our assessment, therefore considering a best case scenario where these individuals are completely protected from infection. The impact of shielding would be strengthened if the target group (70 y.o. and older) was to be extended to those aged 60 y.o. or to younger individuals with comorbidities. However, a lot of individuals aged 60-70 y.o. have not retired yet raising feasibility issues; and age has been found to be the primary driver of severity [33–37] so that this would be unlikely to change our key conclusions. We found similar patterns running a sensitivity analysis including the population of elderly homes in our study population.

Fortunately, the advent of safe and effective vaccines has greatly expanded our toolkit for epidemic control beyond non-pharmaceutical measures. The progressive roll-out of vaccines has reduced the COVID-19 burden by protecting elderly individuals from severe outcomes and by reducing viral circulation [38,39]. Interestingly, we found similarities between the question of vaccine doses' prioritization towards different age groups and that of contact reduction explored here. Modelling studies have highlighted that, if vaccines are highly effective against infection,

vaccinating young adults could be the best way to minimize mortality in a low transmission setting. However, as transmission increases, the optimal strategy switches to vaccinating older individuals [38–40]. This is consistent with our assessment of how optimal target groups may change with R_{eff}.

Case data can be difficult to interpret as they are sensitive to (i) changes in testing capacities and policies and (ii) age-specific characteristics (e.g. propensity to get tested or probability to develop symptoms). In this study, we propose a modelling framework relying on the analysis of the dynamics of the proportion of positive tests among individuals reporting symptoms upon getting tested. Our approach accommodates for temporal changes in the number of tests being performed and age-specific probabilities to be detected (associated with the probability to develop a clinical form of COVID-19) and assumes a constant prevalence of symptoms suggestive of COVID-19 that cannot be attributed to a SARS-CoV-2 infection. Using this framework to study the epidemics during wintertime where other respiratory viruses might be circulating would require further development.

While shielding older individuals can reduce COVID-19 mortality and morbidity, the intervention would not allow an important relaxation of control measures for other age groups in the absence of vaccines due to the porosity of SARS-CoV-2 transmission across age groups. Pandemic control requires an effort from all age groups.

Methods

Hospitalization data

We use hospitalization data extracted from the SI-VIC database. This database is maintained by the ANS (Agence du Numérique en Santé) and provides real time information on the COVID-19 patients hospitalized in public and private French hospitals. Data, including age, hospitalization date, outcome and region, are sent daily to Santé Publique France, the French national public health agency. All COVID-19 cases are either biologically confirmed or present with a computed tomographic image highly suggestive of SARS-CoV-2 infection. Missing ages are imputed assuming that the age distribution of newly hospitalized patients for a given week in a given region is similar to the age distribution obtained from patients with age information. Over our study period, the proportion of individuals with missing ages accounted for less than 0.5% of hospitalizations. We restrict our analysis to patients that are hospitalized in general ward beds (*Hospitalisation conventionnelle*) or ICU beds (*Hospitalisation réanimatoire: réanimation, soins intensifs et unité de surveillance continue*) and discard patients that are hospitalized in emergency care units (*Soins d'urgence*), psychiatric care (*Hospitalisation psychiatrique*) or long-term and rehabilitation care (*Soins de suite et réadaptation*). We consider events (hospitalizations, transfers, deaths or discharges) by date of occurrence and correct observed data for reporting delays [1].

Test data

SIDEP (Système d'Information de Dépistage Populationnel - Information system for population-based testing) is a national surveillance system describing RT-PCR and antigen tests results for SARS-CoV-2 arising from all private and public French laboratories. For the time window used in

this analysis (see Supplementary materials), antigen tests were not included in the database. Anonymized data are transmitted daily to Santé Publique France, the French national public health agency, through a secured platform. Upon testing, individuals are asked to report whether they are experiencing symptoms. Test results are reported by date of nasopharyngeal swab and include patient information such as age, delay since symptoms onset and postal code of the home address. When the home address is not available, the postal code of the lab performing testing is indicated. In case of multiple swabs for a single patient, if test results are both positive and negative, the first test with positive results is kept. If all test results are negative, the results of the first test are kept. The number of tests reported in the SIDEP surveillance system for metropolitan France increased throughout summer from 208,214 on the week of 15 June 2020 to 1,115,644 on the week of 14 September 2020 (Figure S29).

Social contact data

We extracted social contact information from SocialCov, an online survey where participants aged ≥18 y.o. are invited to describe the contacts they had during the previous day. In the survey, a contact was defined as either a physical contact (e.g. a kiss or a handshake), or a close contact (e.g. face to face conversation at less than 1 meter). Collected information includes the age of the person involved in the contact and the setting where the contact happened (i.e. work, home, leisure place, or others). In addition, respondents living with one or more minors were asked to provide the same information for one of them. The survey was advertised following the same approach as in [17]. Data were collected in accordance with the regulation in force in France for the protection and security of personal data. The answers of 1295 participants were collected between 30 July and 27 September 2020. To comply with the constraints in the survey design of the COMES-F study [41], used here as the reference for the mixing patterns in France, individuals with more than 40 contacts were excluded from this analysis, reducing the population from an initial number of 1628 to 1550 (including the underaged population). For each age-group 0-9 y.o., 10-19 y.o., 20-29 y.o., 30-39 y.o., 40-49 y.o., 50-59 y.o., 60-69 y.o., 70-79 y.o., and ≥80 y.o., we computed the mean daily number of contacts, see Table S2.

Transmission model

To describe the dynamics of SARS-CoV-2 in the French population and the trajectories of hospitalized patients, we use an age-stratified deterministic compartmental model whose structure follows the one described in Salje et al [1]. In short, infectiousness begins on average 4 days after infection. On average 5 days after infection, infected individuals move to the I compartment. Symptoms onset occurs upon entry into the I compartment for some of the infected individuals. A subset of infected individuals will develop a severe form of the disease and eventually be hospitalized, on average 7 days after developing symptoms. The probability of hospitalization upon infection is age-dependent, as estimated in Salje et al [1]. The model is stratified in $n_{age} = 9$ age groups: 0-9 y.o., 10-19 y.o., 20-29 y.o., 30-39 y.o., 40-49 y.o., 50-59 y.o., 60-69 y.o., 70-79 y.o., and ≥80 y.o. The model describes the spread of SARS-CoV-2 in the

general population and does not account for the specific transmission patterns observed in elderly homes. We thus remove the population of elderly homes from the population of metropolitan France. The model was coded using the *odin* R package [42].

Changes in transmission intensity and contact patterns

Assumptions about contact patterns before 11 May 2020 (i.e. the end of the country-wide lockdown) are similar to the ones used in Salje et al [1]. The contact matrix describing mixing patterns before the implementation of a country-wide lockdown on 17 March 2020 are extracted from the COMES-F survey [41]. During the lockdown, the contact matrix was modified to account for the strict measures put in place. We assume a new change in the reproduction number and in contact patterns on 11 May 2020, when restrictive measures started to be progressively lifted. We also assume another change in transmission on a date that depends on the region (Table S3), in line with the observed increase in the proportion of positive tests at the regional level (Figure 1). For these two post-lockdown time periods, we estimate reproduction numbers ($R_{postLock}$ and $R_{rebound}$) for each region. At the national level, this corresponds to a reproduction number of 2.90 before 17 March 2020 that was subsequently reduced to 0.67 during the lockdown [1].

Modelling contact patterns between the different age-groups

Let ${c_{i,j}}^{baseline}$ denote the mean daily number of contacts that an individual aged i had with an individual aged j in the pre-lockdown period. These values are extracted from the COMES-F survey [41]. Let α_i denote the reduction of contacts for individuals aged i during a time-period of interest. To ensure that the total number of contacts between individuals aged i and individuals aged j is equal to the total number of contacts between individuals aged j and individuals aged i in the population, we assume that the reduction of contacts between age groups i and j is equal to $r_{i,j} = min\,(\alpha_i, \alpha_j)$. The mean daily number of contacts that an individual aged i has with individuals aged j is thus equal to $r_{i,j} \cdot {c_{i,j}}^{baseline}$. As we are working with normalized contact matrices (i.e. contact matrices divided by their maximum eigenvalue), we are only interested in the relative reduction between different age-groups. We thus set: $\alpha_{20-29y} = 1$ and do not constrain the other α_i values to be lower than 1.

We assume that contact patterns changed at two distinct periods: first, with the progressive easing of control measures after 11 May 2020 and second at the time of the epidemic rebound (Table S3). We estimate parameters related to the reduction of contacts for age-groups: 0-9 y.o.;10-19 y.o.; 30-39 y.o.; 40-49 y.o.; 50-59 y.o.; 60-69 y.o.;70-79 y.o.; and ≥80 y.o. for each of the two time-periods. We assume that parameters describing the change in mixing patterns from the easing of the lockdown until the rebound are the same in all regions and that mixing patterns during the rebound are region-specific.

Estimating effective contact rates between age-groups from the modified matrices

Let $C^{rebound} = ({c_{i,j}}^{rebound})$denote the contact matrix estimated for the rebound period. Numerous factors, including changing climate conditions, more outdoor activities or the adoption of protective behaviours such as masks or hand hygiene, can have an impact on the transmission risk associated with a contact with an infected individual (i.e. the transmission rate). We fix the value of the mean daily number of contacts of individuals aged 20-29 y.o. to the one reported in the SocialCov survey during summer. Let $\mu^{SocialCov}$denote the mean daily number of contacts of individuals aged 20-29 y.o. reported in the SocialCov survey [17]. We then estimate the mean daily number of contacts that an individual aged i has with individuals aged j during the rebound period ${c_{i,j}}^{eff}$ by:

$$ {c_{i,j}}^{eff} = \frac{\mu^{SocialCov}}{\sum_j \ {c_{20-29,j}}^{rebound}} \cdot {c_{i,j}}^{rebound} $$

This rescaling enables a direct interpretation of the coefficients ${c_{i,j}}^{eff}$ as a number of daily contacts. The number of effective contacts in age group i can then be derived as: $C^{eff} = \frac{{\mu_{20,29}}^{SocialCov}}{\sum_j \ {c_{20-29,j}}^{rebound}} \cdot \sum_j \ {c_{i,j}}^{rebound}$, which can be interpreted as the model predicted average number of daily contacts between individuals according to age classes. Importantly, the relative contributions of individuals in different age classes are independent of the chosen rescaling.

Statistical framework

Models are calibrated on weekly age-stratified hospital admissions and number of positive tests among symptomatic individuals in a Bayesian Markov Chain Monte Carlo framework. We account for age-specific probabilities to develop symptoms upon SARS-CoV-2 infection and thus the fact that a greater proportion of all infections are detected among symptomatic individuals. From this, we infer region-specific changes in transmission intensity and contact patterns.

To reduce the impact of potential changes in testing policies, we calibrate our model on the proportion of positive tests amongst symptomatic individuals being tested. Let $S_+(t,a)$ and $S_-(t,a)$ denote respectively the number of positive and negative symptomatic individuals in the population of age a at time t. We assume that $S_-(t,a)$ is constant over time. Let $p(a)$ denote the probability of being symptomatic upon SARS-CoV-2 infection amongst individuals aged a. Let $N(a)$ denote the number of individuals aged a. Let $I(t,a)$ denote the number of individuals aged a in compartment I predicted by the model.

The proportion of positive tests among symptomatic individuals of age a that were tested is:

$$ P_+(t,a) \ = \ \frac{S_+(t,a)}{S_+(t,a) \ + \ S_-(t,a)} \ = \ \frac{p(a) \cdot I(t,a)}{p(a) \cdot I(t,a) \ + \ S_-(t,a)} \ = \ \frac{p(a) \cdot I(t,a)}{p(a) \cdot I(t,a) \ + \ \pi_a \cdot N(a)} $$

where π_a (a parameter to be estimated) is the prevalence of symptoms suggestive of COVID-19 that cannot be attributed to a SARS-CoV-2 infection in individuals aged a at time t. We assume that π_a is constant across age-groups and regions as well as over time. We use the notation π to refer to this quantity. The assumption that π is constant over time is broadly motivated by the low levels of circulation for other respiratory viruses during summer [43,44,45]. Furthermore, we assume a three days delay between symptoms onset and testing, in line with the reported delay between symptoms onset and date of test (Figure S30). We use probabilities to develop a symptomatic form of COVID-19 upon infection as a function of age estimated in Davies et al. [21].

Further information about the inference procedure is detailed in the Supplement.

Simulation of intervention strategies targeting single age-groups

We run forward simulations to evaluate the impact of social distancing strategies that reduce contacts in targeted age-groups, starting from the region-specific date of end of calibration. We assume that when an individual reduces his/her contacts, such a reduction is homogeneously distributed across contacts with the different age-groups. For a strategy targeting age-groups a corresponding to a reduction of x contacts, we define a new contact matrix as:

$$C^{interv} = ({c_{i,j}}^{interv}) = (min({\alpha_i}^{interv}, {\alpha_j}^{interv}) \cdot {c_{i,j}}^{eff})$$

With ${\alpha_i}^{interv} = \frac{(\sum_j {c_{a,j}}^{eff}) - x}{(\sum_j {c_{a,j}}^{eff})}$ if $i = a$ and ${\alpha_i}^{interv} = 1$ otherwise.

We explore the impact of such intervention strategies on the peak in new infections, the peak in hospital and ICU admissions, the number of deaths arising after the date of change in contact patterns, as well as the life-years lost and QALYs lost after the date where the intervention reducing the number of contacts is implemented. We run a range of scenarios characterized by the effective reproduction number at the time targeted measures are implemented, which corresponds to the region-specific date of end of calibration (Table S4). Scenarios are simulated until 1 January 2022. For each one of them, we compute the peak in daily new infections, hospitalizations and admissions in ICUs as well as the number of deaths arising from infections occurring after the date of change in contact patterns and the corresponding number of years of life lost and quality-adjusted life-years lost until the end of the simulation (see Supplementary materials). We explore the impact of interventions in all metropolitan French regions except Corsica due to the high uncertainty around estimates.

Parametrization of shielding scenarios

For strategies shielding the elderly population, we evaluate the impact of a reduction of 30% and 50% of contacts in those aged 70 y.o. and above. We also conduct a sensitivity analysis where contacts are reduced in those aged 60 y.o. and older (Figure S5). We considered the shielding of those aged 70 y.o. and above to be a more realistic scenario as (i) a non-negligible fraction of

those aged 60-69 y.o. is not retired and remains in the active population [46], so that reducing contacts in this age group by 50% might be complicated and as (ii) their perception of their own risk of being susceptible to develop a severe form of COVID-19 might be lower [47]. The value of 50% for the reductions in contact was deliberately defined as an "extreme" scenario to assess the impact of shielding. In Auvergne-Rhône-Alpes, we indeed estimated that individuals aged 80 y.o. and older have on average 2.9 (2.4-3.4) effective contacts per day (Figure 2B). A reduction of 50% would bring this number to 1.5 (1.2-1.7). This is below the number of contacts measured during the stringent lockdown implemented in March-May 2020 in metropolitan France [17]. This is also below the mean daily number of contacts measured in the household setting during the pre-pandemic era (1.84 reported in the COMES-F contact survey from Béraud et al. [41]). Reaching such levels of reductions would already appear difficult given (i) the stringency of the first lockdown implemented in March-May 2020 and (ii) the likely limited reduction in contacts within the household in a scenario of extreme shielding where all other contacts are almost removed. We also explored a less stringent shielding scenario, with a reduction of 30% in effective contacts in the elderly population.

Parametrization of targeted strategies

For strategies targeted towards different age groups, we evaluate the impact of (i) an absolute reduction in effective contacts (e.g. 1) or (ii) a relative reduction in effective contacts (e.g. 10%). We report the results of absolute reductions in the main text as they are more directly interpretable. We also present the second in a sensitivity analysis as the same relative effort in the different age groups does not correspond to the same reduction in absolute number of contacts. To give some context, the absolute and relative reduction in number of contacts that would be necessary to go from the levels measured in the SocialCov survey during summer 2020 to the levels measured during the first national lockdown [17] are reported in Figure S13. For example, reductions of 4.8 contacts in the 20-29 y.o. and 2.0 contacts in the 80 y.o. and older would have been necessary to bring the number of contacts in these age groups to levels measured during spring 2020. This would have corresponded to 62% and 56% reductions, respectively. We also present the result of age targeted strategies as a function of the equivalent number of individuals that would need to be put into lockdown to reach such reductions. The corresponding reductions are derived using the SocialCov survey performed during summer 2020 (Table S2) and the one performed during the first lockdown in spring 2020 [17].

Sensitivity analyses

To assess the robustness of our findings, we explore a range of sensitivity analyses:

- → Assuming a different susceptibility to SARS-CoV-2 infection between age-groups [21]
- → Assuming a different susceptibility to SARS-CoV-2 infection and infectivity between age-groups [21]
- → Assuming a lower susceptibility of 0-19 y.o. compared to 20 y.o. and older [19]
- → Including the population of elderly homes in the study population
- → Assuming quadratic reductions in contact patterns (i.e. contact reductions apply both to the contacted and the contacting groups)

- → Assuming contact patterns are only modified outside the household

Further details about the parametrization of the different sensitivity analyses are reported in the Supplement.

Figures

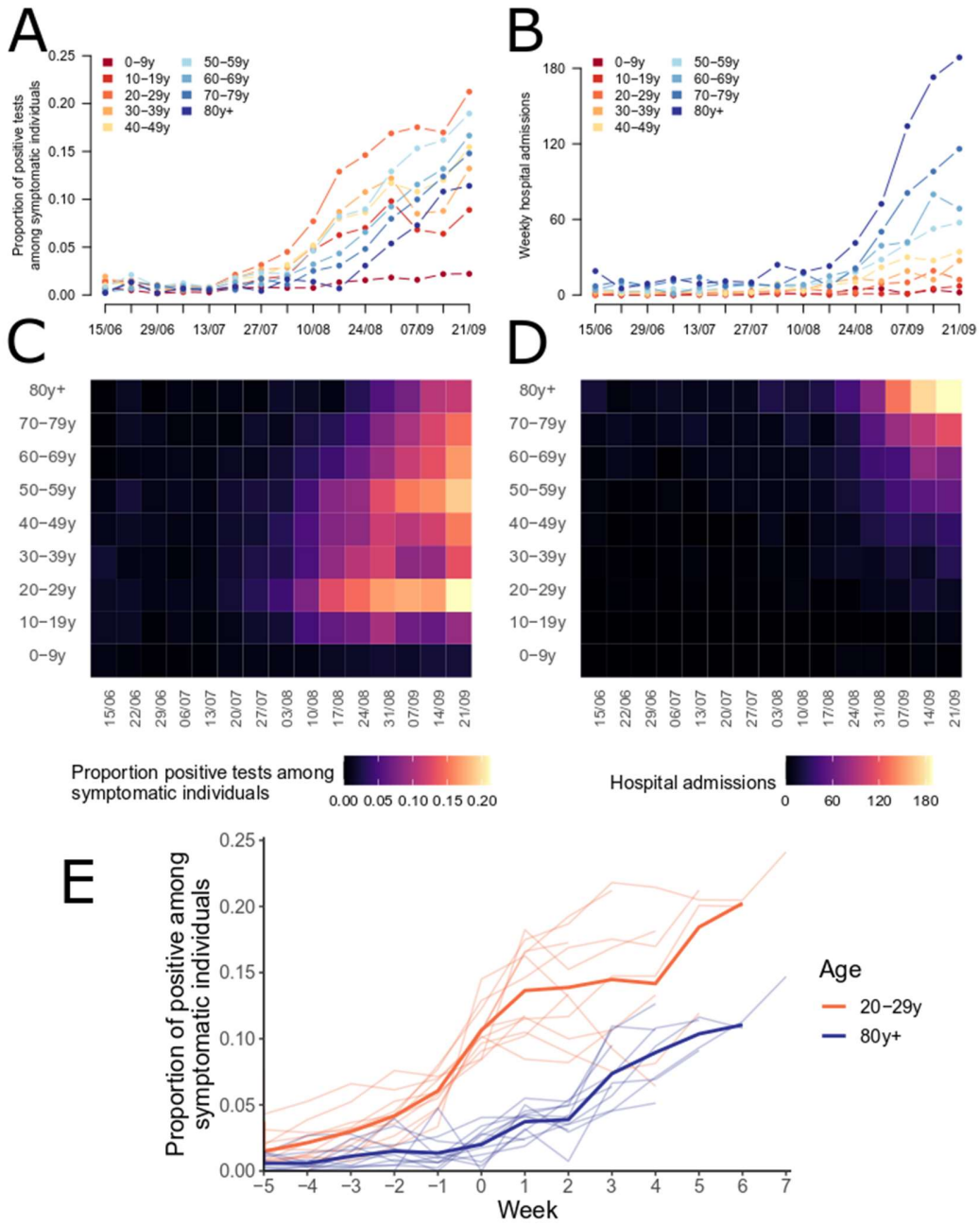

Figure 1: Dynamics of the epidemic rebound by age-group. **(A-B)** Weekly proportion of positive tests amongst symptomatic individuals being tested and **(C-D)** weekly number of hospital admissions, by age group in Auvergne-Rhône-Alpes region. **(E)** Proportion of positive tests among symptomatic individuals in individuals aged 20-29 y.o. and older than 80 y.o. In (E), the light lines represent the trends in the 13 metropolitan French regions. The wider lines indicate the mean proportion of positive among symptomatic across regions. Week 0 corresponds to the first week when the proportion of positive tests among symptomatic individuals aged 20-29 y.o. reaches 8%.

Figure 2

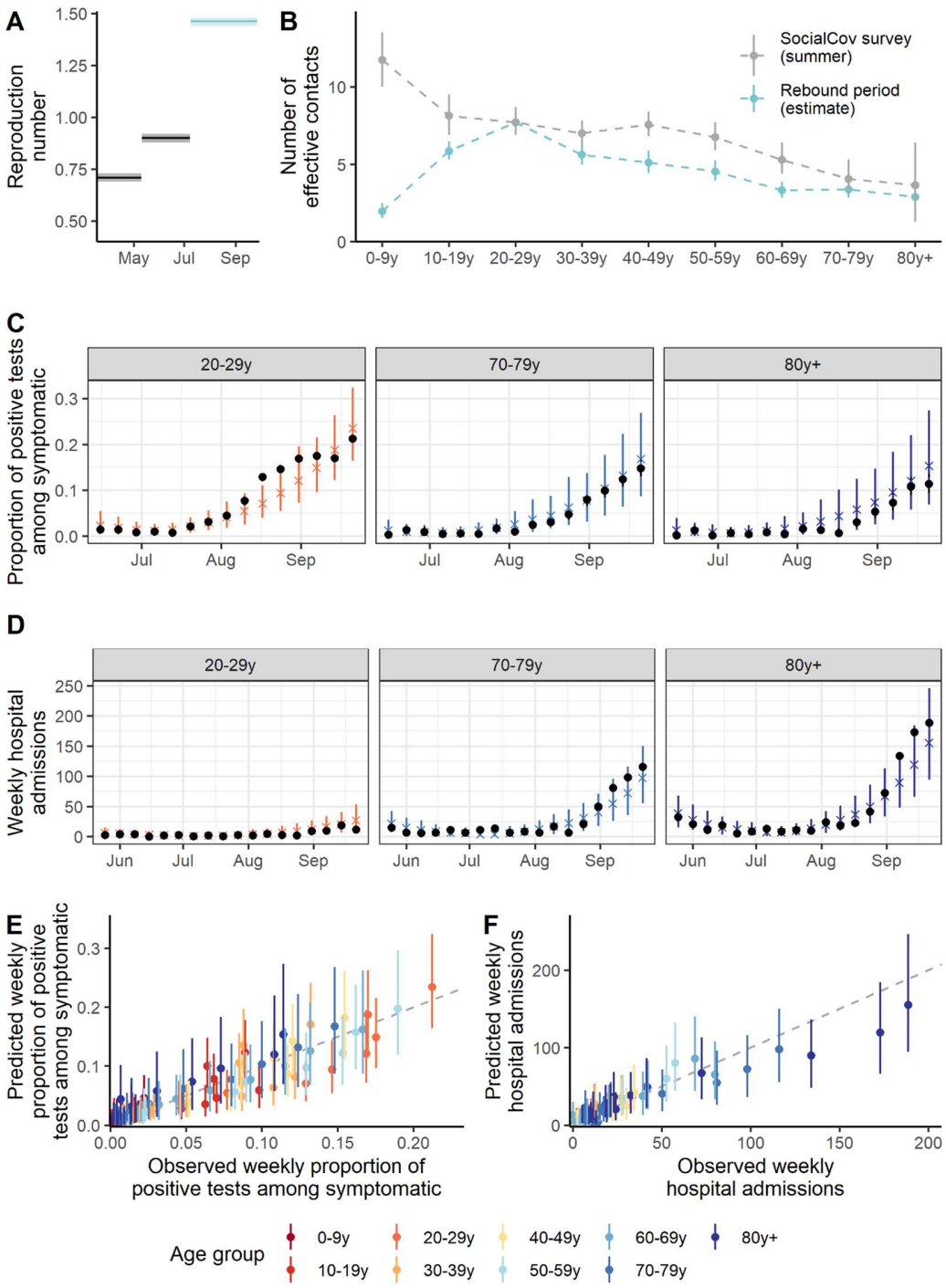

Figure 2: Model predictions for Auvergne-Rhône-Alpes region. (A) Intervention reproduction number estimates during the epidemic. **(B)** Effective number of contact estimated for each age group during the rebound period (9 July - 27 September). **(C)** Predicted and observed weekly proportion of positive tests amongst symptomatic individuals being tested aged 20-29y, 70-79y and 80y+. **(D)** Predicted and observed weekly number of hospitalizations of individuals aged 20-29y, 70-79y and 80y+. **(E)** Predicted and observed weekly proportion of positive tests among

symptomatic individuals being tested. **(F)** Predicted and observed weekly hospital admissions. The black points in (C) indicate the data. The vertical segments for the blue curve in panel (B) correspond to 95% credible intervals and for the grey curve to 95% bootstrap confidence intervals. The vertical segments in panels (C-D) indicate 95% credible intervals. In panels (E-F), each point corresponds to a specific week and age group.

Figure 3

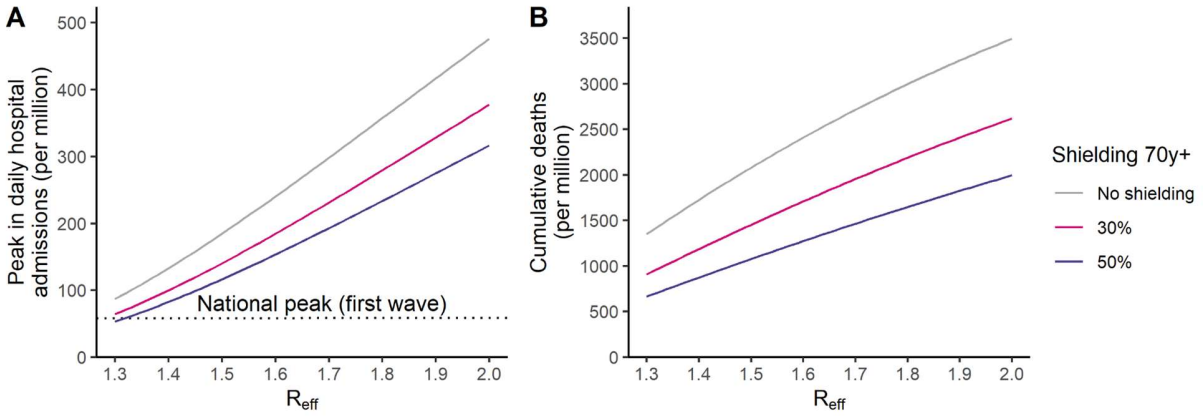

Figure 3: Impact of strategies shielding the elderly population. (A) Peak in hospital admissions per million and **(B)** number of deaths per million as a function of the effective reproduction number R_{eff} assuming a reduction of 50% or 30% in effective contacts of those older than 70 y.o. The number of deaths is computed from the time interventions are implemented until the end of the simulation, corresponding to the period from September 28th, 2020 to January 1st, 2022. The impact of reducing contacts in individuals aged 70 y.o. and older in counterfactual simulations was reported according to the effective reproduction number at the start of the simulation. The effective reproduction number decreased over the course of the simulation with increasing immunity.

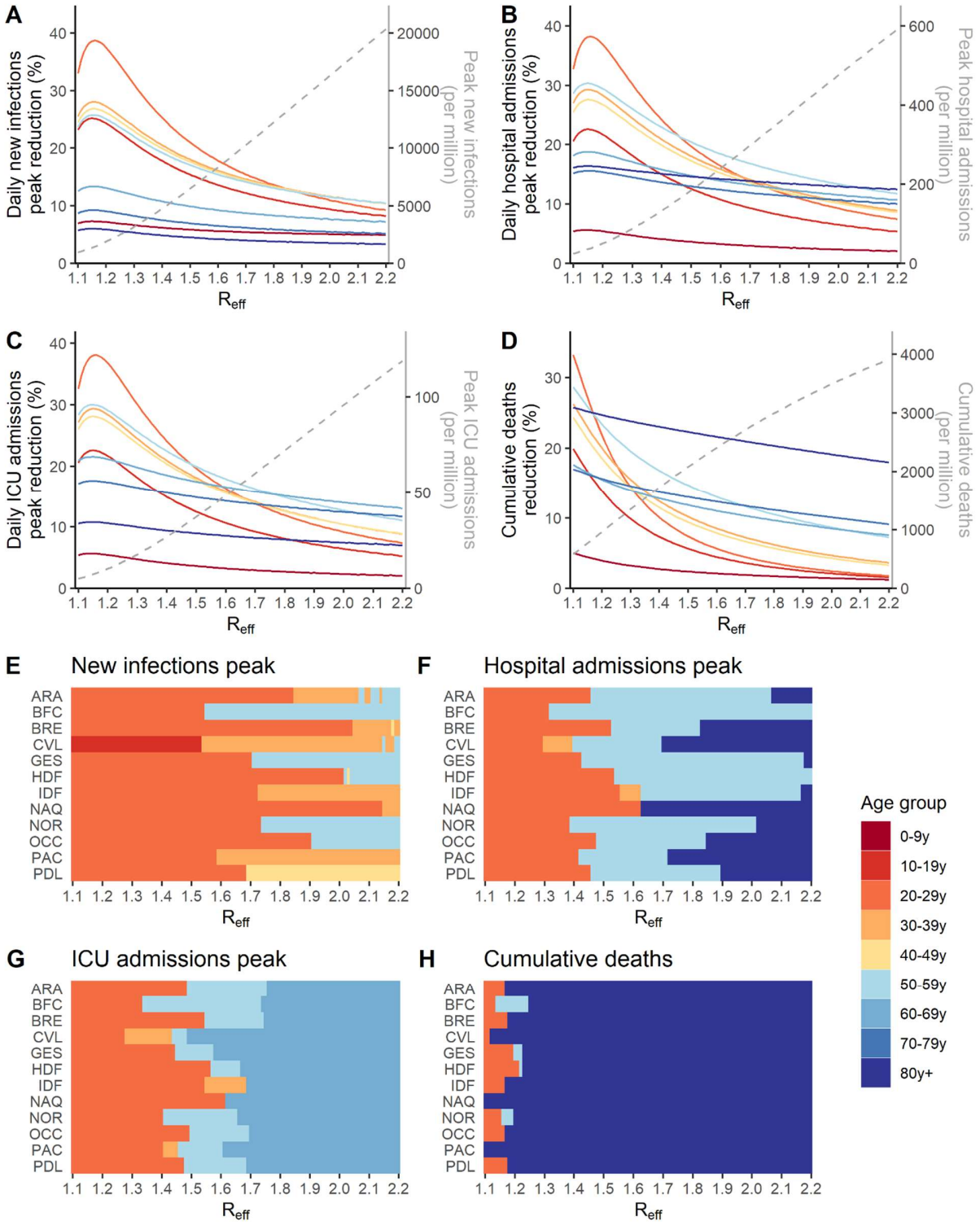

Figure 4: Impact of strategies targeting specific age groups. Reduction in **(A)** the peak in daily new infections, **(B)** the peak in hospital admissions, **(C)** the peak in daily ICU admissions, **(D)** the number of deaths when individuals in the target age group reduce their effective contacts

by 1, as a function of the effective reproduction number R_{eff}, in the Auvergne-Rhône-Alpes region. The grey dotted lines indicate, in the absence of additional measure, the value of the epidemiological metrics. Age-groups for which a reduction of 1 contact results in the highest impact on the reduction of **(E)** the peak in daily new infections, **(F)** the peak in hospital admissions, **(G)** the peak in daily ICU admissions, **(H)** the number of deaths as a function of the effective reproduction number R_{eff}. In counterfactual simulations, the impact of reducing 1 effective daily contacts in each age group from the region-specific date of beginning of simulation (Table S4) to January 1st, 2022 was compared for different values of the effective reproduction numbers at the beginning of the simulations, which then declined in the simulation with increasing immunity. The number of deaths is computed from the time interventions are implemented until the end of the simulation. Region's abbreviations are detailed in supplementary text.

Figure 5

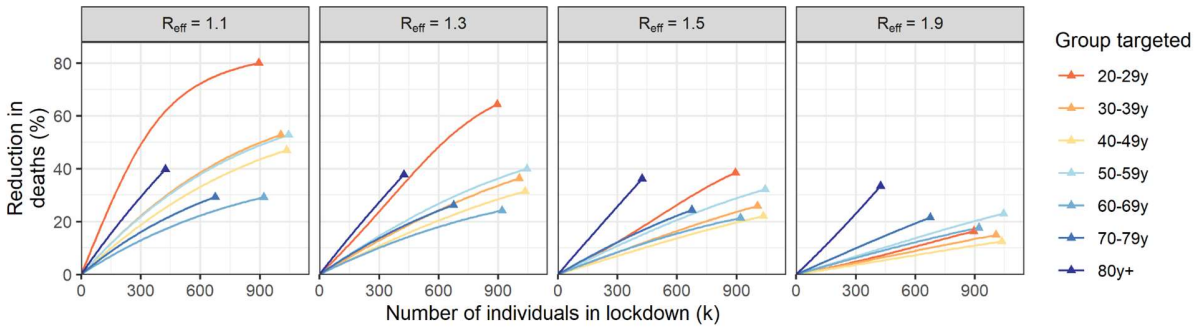

Figure 5: Impact of targeted strategies as a function of the equivalent number of individuals put into lockdown in the different age groups. Percentage reduction in cumulative deaths in the Auvergne-Rhône-Alpes region for strategies targeting different age groups. Results are presented for different values of the effective reproduction number R_{eff} at the beginning of the simulations, which then declined in the simulation with increasing immunity. Simulations are run for different intensities of targeting. For each targeted strategy, we compute the equivalent number of individuals that would need to be put into lockdown to reach this level. The lockdown of an entire age group corresponds to the triangle.

Figure 6

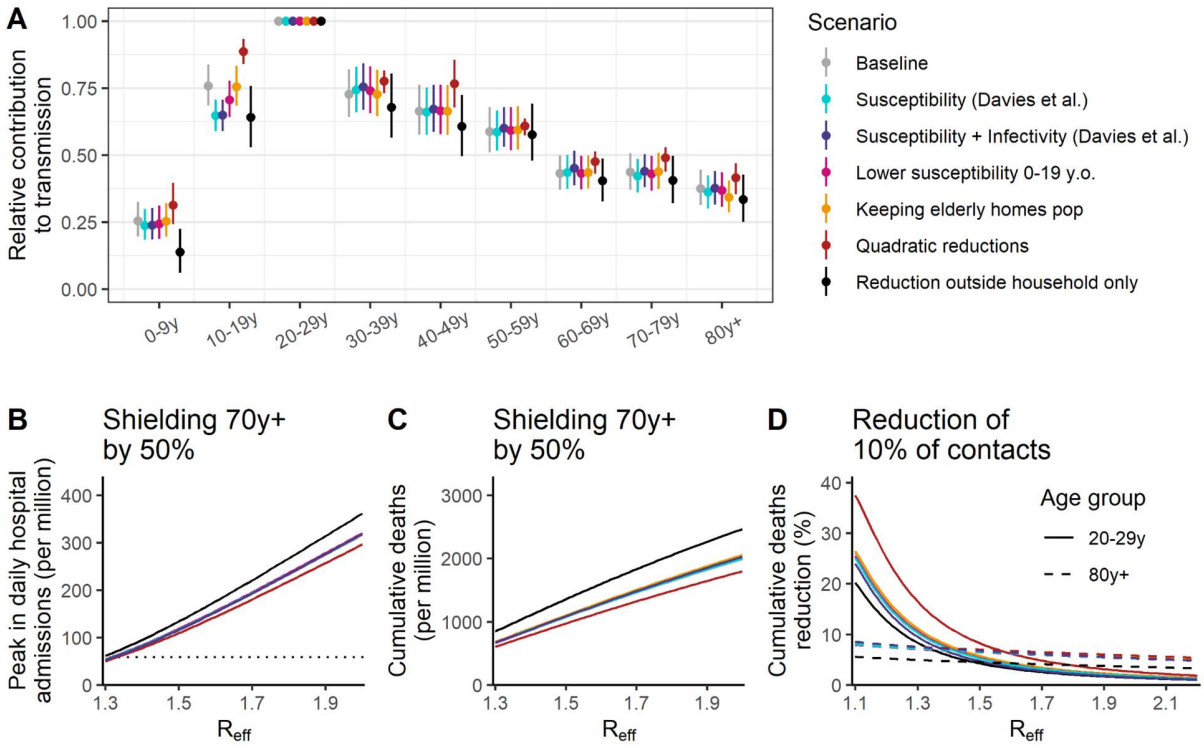

Figure 6: Sensitivity analyses for the Auvergne-Rhône-Alpes region. (A) Relative contribution of the different age groups to transmission compared to the 20-29 y.o. age group across a range of scenarios. **(B)** Peak in daily hospital admissions (per million inhabitants) assuming a reduction of 50% in contacts of those older than 70 y.o. across a range of scenarios as a function of the effective reproduction number R_{eff}. **(C)** Number of deaths (per million inhabitants) assuming a reduction of 50% in contacts of those older than 70 y.o. across a range of scenarios as a function of the effective reproduction number R_{eff}. **(D)** Reduction in the number of deaths (reported in percentage) as a function of the effective reproduction number R_{eff} for strategies targeting those aged 20-29 y.o. and those 80 y.o. and older. The horizontal dotted line in panel B corresponds to the peak in daily hospital admissions observed at the national level during the first pandemic wave of SARS-CoV-2. The scenarios explored are: *Susceptibility (Davies et al.)* - Using age-specific susceptibilities [21] ; *Susceptibility + Infectivity (Davies et al.)* - Using age-specific susceptibilities and infectivities [21]; *Lower susceptibility 0-19 y.o.* - 0-9 y.o. and 10-19 y.o. are respectively 50% and 25% less susceptible to SARS-CoV-2 infection than 20 y.o. and older ; *Keeping elderly homes pop* - Including the population of elderly homes in the study population ; *Quadratic reduction* - Considering quadratic reductions in contact patterns ; *Reduction outside household only* - Assuming contact patterns are only modified outside the household. In counterfactual simulations, the impact of the targeted strategies from September 28th, 2020 to January 1st, 2022 was compared for varying, counterfactual degrees in effective reproduction numbers at the beginning of the simulations, which then declined in the simulation with increasing immunity.

References

1. Salje, H. *et al.* Estimating the burden of SARS-CoV-2 in France. *Science* **369**, 208–211 (2020).
2. Flaxman, S. *et al.* Estimating the effects of non-pharmaceutical interventions on COVID-19 in Europe. *Nature* **584**, 257–261 (2020).
3. Great Barrington Declaration. https://gbdeclaration.org/.
4. Hoertel, N. *et al.* A stochastic agent-based model of the SARS-CoV-2 epidemic in France. *Nature Medicine* vol. 26 1417–1421 (2020).
5. Alwan, N. A. *et al.* Scientific consensus on the COVID-19 pandemic: we need to act now. *Lancet* **396**, e71–e72 (2020).
6. Archer, S. L. 5 failings of the Great Barrington Declaration's dangerous plan for COVID-19 natural herd immunity. *The Conversation* (2020).
7. expert reaction to Barrington Declaration, an open letter arguing against lockdown policies and for 'Focused Protection'. *Science Media Scentre*.
8. Miller, M. A. *et al.* Prioritization of influenza pandemic vaccination to minimize years of life lost. *J. Infect. Dis.* **198**, 305–311 (2008).
9. Wallinga, J., van Boven, M. & Lipsitch, M. Optimizing infectious disease interventions during an emerging epidemic. *Proc. Natl. Acad. Sci. U. S. A.* **107**, 923–928 (2010).
10. Longini, I. M. *et al.* Estimation of the efficacy of live, attenuated influenza vaccine from a two-year, multi-center vaccine trial: implications for influenza epidemic control. *Vaccine* **18**, 1902–1909 (2000).
11. Piedra, P. A. *et al.* Herd immunity in adults against influenza-related illnesses with use of the trivalent-live attenuated influenza vaccine (CAIV-T) in children. *Vaccine* **23**, 1540–1548 (2005).

12. Reichert, T. A. *et al.* The Japanese experience with vaccinating schoolchildren against influenza. *N. Engl. J. Med.* **344**, 889–896 (2001).
13. Monto, A. S., Davenport, F. M., Napier, J. A. & Francis, T., Jr. Effect of vaccination of a school-age population upon the course of an A2-Hong Kong influenza epidemic. *Bull. World Health Organ.* **41**, 537–542 (1969).
14. Baden, L. R. *et al.* Efficacy and Safety of the mRNA-1273 SARS-CoV-2 Vaccine. *N. Engl. J. Med.* **384**, 403–416 (2021).
15. Voysey, M. *et al.* Single-dose administration and the influence of the timing of the booster dose on immunogenicity and efficacy of ChAdOx1 nCoV-19 (AZD1222) vaccine: a pooled analysis of four randomised trials. *Lancet* **397**, 881–891 (2021).
16. Polack, F. P. *et al.* Safety and Efficacy of the BNT162b2 mRNA Covid-19 Vaccine. *New England Journal of Medicine* vol. 383 2603–2615 (2020).
17. Bosetti, P. *et al.* Lockdown impact on age-specific contact patterns and behaviours in France. (2020) doi:10.1101/2020.10.07.20205104.
18. Goldstein, E., Lipsitch, M. & Cevik, M. On the effect of age on the transmission of SARS-CoV-2 in households, schools and the community. *medRxiv* (2020) doi:10.1101/2020.07.19.20157362.
19. Viner, R. M. *et al.* Susceptibility to SARS-CoV-2 Infection Among Children and Adolescents Compared With Adults: A Systematic Review and Meta-analysis. *JAMA Pediatr.* **175**, 143–156 (2021).
20. Zhu, Y. *et al.* A Meta-analysis on the Role of Children in Severe Acute Respiratory Syndrome Coronavirus 2 in Household Transmission Clusters. *Clin. Infect. Dis.* **72**, e1146–e1153 (2021).
21. Davies, N. G. *et al.* Age-dependent effects in the transmission and control of COVID-19 epidemics. *Nature Medicine* vol. 26 1205–1211 (2020).
22. Santé Publique France. *COVID-19 : point épidémiologique du 15 octobre 2020*.

https://www.santepubliquefrance.fr/maladies-et-traumatismes/maladies-et-infections-respiratoires/infection-a-coronavirus/documents/bulletin-national/covid-19-point-epidemiologique-du-15-octobre-2020 (2020).

23. Santé Publique France. *COVID-19 : point épidémiologique du 22 octobre 2020*. https://www.santepubliquefrance.fr/maladies-et-traumatismes/maladies-et-infections-respiratoires/infection-a-coronavirus/documents/bulletin-national/covid-19-point-epidemiologique-du-22-octobre-2020 (2020).
24. Santé Publique France. *COVID-19 : point épidémiologique du 29 octobre 2020*. https://www.santepubliquefrance.fr/maladies-et-traumatismes/maladies-et-infections-respiratoires/infection-a-coronavirus/documents/bulletin-national/covid-19-point-epidemiologique-du-29-octobre-2020 (2020).
25. Oster, A. M., Caruso, E., DeVies, J., Hartnett, K. P. & Boehmer, T. K. Transmission Dynamics by Age Group in COVID-19 Hotspot Counties - United States, April-September 2020. *MMWR Morb. Mortal. Wkly. Rep.* **69**, 1494–1496 (2020).
26. Lau, M. S. Y. *et al.* Characterizing superspreading events and age-specific infectiousness of SARS-CoV-2 transmission in Georgia, USA. *Proc. Natl. Acad. Sci. U. S. A.* **117**, 22430–22435 (2020).
27. Monod, M. *et al.* Age groups that sustain resurging COVID-19 epidemics in the United States. *Science* **371**, (2021).
28. Clarfield, A. M. & Jotkowitz, A. Age, ageing, ageism and 'age-itation' in the Age of COVID-19: rights and obligations relating to older persons in Israel as observed through the lens of medical ethics. *Isr. J. Health Policy Res.* **9**, 64 (2020).
29. Piccoli, M., Tannou, T., Hernandorena, I. & Koeberle, S. [Ethical approach to the issue of confinement of the elderly in the context of the COVID-19 pandemic: Prevention of frailty versus risk of vulnerability]. *Ethics Med Public Health* **14**, 100539 (2020).
30. Beauchamp, T. L. & Childress, J. F. *Principles of biomedical ethics. 5th ed*. ({Oxford

University Press}, 2021).

31. O'Driscoll, M. *et al.* Age-specific mortality and immunity patterns of SARS-CoV-2. *Nature* **590**, 140–145 (2021).
32. Direction de la Recherche, des Études, de l'Évaluation et des Statistiques (DREES) - Ministère de la Santé. Enquête auprès des établissements d'hébergement pour personnes âgées (EHPA) - 2015. (2015).
33. Williamson, E. J. *et al.* Factors associated with COVID-19-related death using OpenSAFELY. *Nature* **584**, 430–436 (2020).
34. Boulle, A. *et al.* Risk factors for COVID-19 death in a population cohort study from the Western Cape Province, South Africa. *Clin. Infect. Dis.* (2020) doi:10.1093/cid/ciaa1198.
35. Docherty, A. B. *et al.* Features of 20 133 UK patients in hospital with covid-19 using the ISARIC WHO Clinical Characterisation Protocol: prospective observational cohort study. *BMJ* **369**, m1985 (2020).
36. Tartof, S. Y. *et al.* Obesity and Mortality Among Patients Diagnosed With COVID-19: Results From an Integrated Health Care Organization. *Ann. Intern. Med.* **173**, 773–781 (2020).
37. Gupta, S. *et al.* Factors Associated With Death in Critically Ill Patients With Coronavirus Disease 2019 in the US. *JAMA Intern. Med.* **180**, 1436–1447 (2020).
38. Tran Kiem, C. *et al.* A modelling study investigating short and medium-term challenges for COVID-19 vaccination: From prioritisation to the relaxation of measures. *EClinicalMedicine* **38**, 101001 (2021).
39. Bubar, K. M. *et al.* Model-informed COVID-19 vaccine prioritization strategies by age and serostatus. *Science* **371**, 916–921 (2021).
40. Hogan, A. B. *et al.* Within-country age-based prioritisation, global allocation, and public health impact of a vaccine against SARS-CoV-2: A mathematical modelling analysis. *Vaccine* **39**, 2995–3006 (2021).

41. Béraud, G. *et al.* The French Connection: The First Large Population-Based Contact Survey in France Relevant for the Spread of Infectious Diseases. *PLoS One* **10**, e0133203 (2015).
42. FitzJohn, R. ODE Generation and Integration [R package odin version 1.2.1]. (2021).
43. Gaunt, E. R., Hardie, A., Claas, E. C. J., Simmonds, P. & Templeton, K. E. Epidemiology and clinical presentations of the four human coronaviruses 229E, HKU1, NL63, and OC43 detected over 3 years using a novel multiplex real-time PCR method. *J. Clin. Microbiol.* **48**, 2940–2947 (2010).
44. Visseaux, B. *et al.* Prevalence of respiratory viruses among adults, by season, age, respiratory tract region and type of medical unit in Paris, France, from 2011 to 2016. *PLoS One* **12**, e0180888 (2017).
45. Casalegno, J.-S. *et al.* Characteristics of the delayed respiratory syncytial virus epidemic, 2020/2021, Rhône Loire, France. *Euro Surveill.* **26**, (2021).
46. DRESS. Les retraités et les retraites - édition 2021. https://drees.solidarites-sante.gouv.fr/publications-documents-de-reference/panoramas-de-la-drees/les-retraites-et-les-retraites-edition-0.
47. Bruine de Bruin, W. Age Differences in COVID-19 Risk Perceptions and Mental Health: Evidence From a National U.S. Survey Conducted in March 2020. *J. Gerontol. B Psychol. Sci. Soc. Sci.* **76**, e24–e29 (2021).
48. Diekmann, O., Heesterbeek, J. A. & Metz, J. A. On the definition and the computation of the basic reproduction ratio R0 in models for infectious diseases in heterogeneous populations. *J. Math. Biol.* **28**, 365–382 (1990).
49. Lefrancq, N. *et al.* Evolution of outcomes for patients hospitalised during the first 9 months of the SARS-CoV-2 pandemic in France: A retrospective national surveillance data analysis. *The Lancet Regional Health - Europe* vol. 5 100087 (2021).
50. Insee − Institut national de la statistique et des études économiques. https://www.insee.fr/.

51. Chevalier, J. & de Pouvourville, G. Valuing EQ-5D using time trade-off in France. *Eur. J. Health Econ.* **14**, 57–66 (2013).
52. Sandmann, F. *et al.* The potential health and economic value of SARS-CoV-2 vaccination alongside physical distancing in the UK: transmission model-based future scenario analysis and economic evaluation. doi:10.1101/2020.09.24.20200857.
53. van Hoek, A. J., Underwood, A., Jit, M., Miller, E. & Edmunds, W. J. The impact of pandemic influenza H1N1 on health-related quality of life: a prospective population-based study. *PLoS One* **6**, e17030 (2011).
54. Baguelin, M., Camacho, A., Flasche, S. & John Edmunds, W. Extending the elderly- and risk-group programme of vaccination against seasonal influenza in England and Wales: a cost-effectiveness study. *BMC Medicine* vol. 13 (2015).
55. Cuthbertson, B. H., Roughton, S., Jenkinson, D., Maclennan, G. & Vale, L. Quality of life in the five years after intensive care: a cohort study. *Crit. Care* **14**, R6 (2010).
56. Griffiths, J. *et al.* An exploration of social and economic outcome and associated health-related quality of life after critical illness in general intensive care unit survivors: a 12-month follow-up study. *Critical Care* vol. 17 R100 (2013).
57. Li, R. *et al.* Substantial undocumented infection facilitates the rapid dissemination of novel coronavirus (SARS-CoV-2). *Science* **368**, 489–493 (2020).
58. Zhang, J. *et al.* Changes in contact patterns shape the dynamics of the COVID-19 outbreak in China. *Science* **368**, 1481–1486 (2020).

Data availability: Data (including regional test and hospitalization data used for the inference) used in the analysis is available at: gitlab.pasteur.fr/mmmi-pasteur/agedynamics_sarscov2 .

Code availability: The code used to calibrate the model and run forward simulations is available at: gitlab.pasteur.fr/mmmi-pasteur/agedynamics_sarscov2 .

Acknowledgments: We acknowledge financial support from the Investissement d'Avenir program, the Laboratoire d'Excellence Integrative Biology of Emerging Infectious Diseases program (grant ANR-10-LABX-62-IBEID), Santé Publique France, the INCEPTION project

(PIA/ANR-16-CONV-0005), the European Union's Horizon 2020 research and innovation program under grant 101003589 (RECOVER) and 874735 (VEO), AXA and Groupama.

Author contributions: CTK and SC conceived the study. CTK, PB, JP, PC, HS, NL and LO performed the analyses. CTK and SC wrote the first draft. All authors contributed to revisions of the manuscript.

Competing interests: None declared

Supplementary information

Supplementary materials

Supplementary text

Figures S1 to S31

Tables S1 to S7

Supplementary materials

Estimating the lag between the increase in the proportion of positive tests in 20-29 y.o. and in those 80 y.o. and older

To compute the lag between the increase in the proportion of positive tests in 20-29 y.o. and in 80 y.o. and older, we defined for each region the origin of time as the first week for which the proportion of symptomatic tests among symptomatic individuals reaches 8%. We then calculate the mean of the proportion of positive amongst symptomatic in 20-29 y.o. and in 80 y.o. and older across all regions. We then compute the lag by minimizing the sum of squared errors between the curves. The sum of squared errors is computed over weeks for which at least 5 regions reached the mean proportion.

Time window used for the model calibration

The SIDEP system was initiated on 13 May 2020 with a progressive increase in the number of laboratories reporting the results (from 4562 on the week of 13 May 2020 to 5447 on the week of 15 June 2020) (Figure S31). On the week of 13 May 2020, 17.2% of individuals with a positive test result (without missing information about the presence/absence of symptoms) reported developing symptoms more than 2 weeks prior to the test. From the week of 15 June 2020, this proportion was down to 1.0%. From the week of 15 June 2020, the number of laboratories reporting results in the SIDEP database remains quite stable. From this date, the proportion of tested individuals with a delay between symptoms onset and test greater than 2 weeks also remained constant (Figure S29). We thus begin the calibration of our model on test data on the week of 15 June 2020. We fitted our model to the proportion of positive tests among symptomatic individuals as this quantity is most likely less sensitive to contact tracing efficiency in a period where the circulation of other respiratory viruses remains low [44].

Following the increase in the number of positive tests and hospital admissions, control measures have progressively been implemented in some regions, resulting in a decrease in the reproduction number (e.g. Provence-Alpes Côte d'Azur region). As we aim to describe transmission patterns during summer before the implementation of additional measures, we define region-specific final date of calibration (the latest possible date being 27 September 2020) based on the time-trends of the proportion of positive tests among symptomatic individuals (Table S4).

The age distribution of hospital admissions predicted by our model depends on our assumptions about mixing patterns. Due to the delay between infection and hospital admissions, individuals admitted to hospital during the two weeks following lockdown release will have mostly been infected during the lockdown period. As we fix the contact matrix describing age-specific contact patterns during the lockdown, we only begin the calibration of our model on age-stratified data on 25 May 2020 (i.e. 2 weeks after the end of the country-wide lockdown). Between 11 May 2020 and 24 May 2020, we calibrate our model on the daily number of hospital admissions occurring in each metropolitan French region.

Models are calibrated using SI-VIC data (extracted from the SI-VIC database on 12 October 2020) between 11 May 2020 and the region-specific final date of calibration and on the weekly proportion of positive tests among individuals reporting symptoms (extracted from SIDEP data) between 15 June 2020 and the region-specific final date of calibration.

Computing the effective reproduction number in an age-structured population

The basic reproduction number R_0 corresponds to the average number of infections resulting from a typical index case in a completely susceptible population in the absence of intervention. We introduce the intervention reproduction number R_i to describe the impact of interventions, behavioural changes or climatic conditions on the value of the transmission rate. This value corresponds to the average number of infections resulting from a typical index case that would be observed in a completely susceptible population under a given set of interventions. The effective reproduction number R_{eff} accounts for the fact that a fraction of the population is immune and no longer contributes to the infection spread. To compute the effective reproduction number, we use the next-generation matrix approach [48]. Let ${p_S}^i(t)$ denote the proportion of the population aged i susceptible to infection at time t. Let $c_{i,j}$ denote the mean daily number of contacts that and individual aged i has with someone aged j.

The effective reproduction number is then derived as:

$R_{eff}(t) = R_i \cdot \rho(\ [c_{i,j} \cdot {p_S}^j(t)]_{ij}\ )\ /\ \rho(\ [c_{i,j}]_{ij}\ )$ where $\rho(M)$denotes the spectral radius of a matrix M.

Statistical framework

Models are calibrated using SI-VIC data (extracted from the SI-VIC database on 12 October 2020) between 11 May 2020 and the region-specific final date of calibration and on the weekly proportion of positive tests among individuals reporting symptoms (extracted from SIDEP data) between 15 June 2020 and the region-specific final date of calibration (see Supplementary materials). Parameters are estimated using a Bayesian Markov Chain Monte Carlo framework. We develop a Metropolis-Hastings algorithm with lognormal proposals and uniform priors for all the parameters. Chains are run with 100,000 iterations removing 5,000 iterations of burn-in.

Let $Adm_{hos}{}^{obs}(t)$ and ${Adm_{hosp}}^{pred}(t)$ denote the observed and expected number of COVID-19 hospital admissions on day t for the whole population. After 24 May 2020, age-groups are specifically considered and data are aggregated at the week level. Let ${Adm_{hosp}}^{obs}(w,a)$ and ${Adm_{hosp}}^{pred}(w,a)$ denote the observed and predicted number of COVID-19 patients belonging to age group a admitted to hospital on week w. Let $X^{obs}(w,a)$ and $N^{obs}(w,a)$ denote the number of positive tests and the number of tests amongst symptomatic individuals being tested on week w in age-group a. Let ${P_+}^{pred}(w,a)$ denote the proportion of positive tests amongst symptomatic

individuals tested predicted by the model for age group a on week w. The likelihood function until day T is then defined as:

$$L_T = L^{hosp}(T) \cdot L^{Age-Hosp}(T) \cdot L^{Age-Tests}(T)$$

with:

$$L^{hosp}(T) = \prod_{t=11\,May}^{24\,May} g_{\delta_1}(Adm_{hosp}{}^{obs}(t) | Adm_{hosp}{}^{pred}(t))$$

$$L^{Age-Hosp}(T) = \prod_{w=w_1}^{w_T} \prod_{a=1}^{n_{age}} g_{\delta_2}(Adm_{hosp}{}^{obs}(w,a) | Adm_{hosp}{}^{pred}(w,a))$$

$$L^{Age-Tests}(T) = \prod_{w=w_2}^{w_T} \prod_{a=1}^{n_{age}} g_{\delta_3}(X^{obs}(w,a) | N^{obs}(w,a) \cdot P_+{}^{pred}(w,a))$$

Where w_1 corresponds to the week starting on 25 May 2020, w_T corresponds to the week of time T, w_2 corresponds to the first week for which we consider test data to be reliable (15 June 2020), $g_\delta(\cdot|X)$ is a negative binomial distribution of mean X and overdispersion parameter X^δ. n_{age} corresponds to the number of age groups in the model. δ_2 and δ_3 are overdispersion parameters to be estimated. δ_1 is the value of the overdispersion parameter estimated during the first wave of SARs-CoV-2 in France [1].

Computing age-specific probability of ICU admission and death given hospitalization

To capture changes in the probability of ICU admission given hospitalisation and death given hospitalisation of COVID-19 patients in Metropolitan France [49], we compute updated estimates from the proportion of patients in the different age groups that have been admitted in ICU or that died in September-October 2020 reported in the SI-VIC surveillance system (Table S5). Using the same approach, we compute the proportion of deaths that occur in ICU in the different age groups (Table S6).

Computing the peak in ICU admissions, the number of deaths, years of life lost and quality adjusted years of life lost arising from infections occurring after the date of change in contacts patterns

Based on the age-specific probabilities of death given hospitalization estimated between 13 July 2020 and 30 September 2020 (Table S5), we compute the number of deaths arising from infections occurring after the date of change in contact patterns and the corresponding number of years of life lost until the end of the simulation. Life expectancies for a given age group were computed using data from the National Institute for Statistics and Economic Studies (Institut national de la statistique et des études économiques - INSEE) [50]. We also compute the quality adjusted years of life lost arising from infections occurring after the date of change in contact patterns. We use age-specific utilities derived for the French setting [51]. We follow the approach proposed by Sandmann et al. [52] to derive the quality-adjusted life years (QALYs) loss per

symptomatic cases, non-fatal hospitalized cases in general wards et non-fatal hospitalized cases admitted in ICUs. We assume that a symptomatic case results in a loss of 0.008 QALYs [53], a non-fatal hospitalization in general ward beds in a loss of 0.018 QALYs [53,54] and a non-fatal ICU hospitalization in a loss of 0.15 QALYs [55,56]. To compute the number of symptomatic infections, we use the age-specific proportion of clinical infections, as estimated in Davies et al [21]. The corresponding weights used to compute the number of life years lost and quality adjusted life years lost arising from deaths are reported in Table S7.

Sensitivity analyses - rationale and description

In the following paragraph, we detail the different sensitivity analyses that we explore alongside a rationale for considering each of them:

→ **Assuming a different susceptibility to SARS-CoV-2 infection between age-groups**

In our baseline scenario, we do not account for a different susceptibility of the different age groups to SARS-CoV-2 infection. In a sensitivity analysis, we explore a scenario with different susceptibilities, using the values estimated by Davies et al. [21]. Let σ_i denote the susceptibility of age group i. For a contact matrix $(c_{i,j})_{i,j}$ describing the average daily number of contacts that individuals of age group i have with individuals of age group j, we modify the coefficients as $(\sigma_i \cdot c_{i,j})_{i,j}$ to account for the susceptibility as a function of age.

→ **Assuming a different susceptibility to SARS-CoV-2 infection and infectivity between age-groups**

In our baseline scenario, we do not account for a different susceptibility of the different age groups to SARS-CoV-2 infection nor for a different infectivity across the different age groups. In a sensitivity analysis, we explore a scenario with different susceptibilities, using the values estimated by Davies et al. [21] and different infectivities for the different age groups. Let σ_i (respectively θ_i) denote the susceptibility (respectively the infectivity) of age group i. For a contact matrix $(c_{i,j})_{i,j}$ describing the average daily number of contacts that individuals of age group i have with individuals of age group j, we modify the coefficients as $(\sigma_i \cdot c_{i,j} \cdot \theta_j)_{i,j}$ to account for susceptibility and infectivity as a function of age. To compute values of the infectivity for different age groups, we assume that symptomatic individuals are more infectious than asymptomatic individuals and that their probability of transmission upon contact with a susceptible individual is $\theta_{asympto} = 55\%$ that of symptomatic individuals [57]. The infectivity of age group j can then be derived as: $\theta_j = {p_j}^{sympto} \cdot (1 - \theta_{asympto}) + \theta_{asympto}$ where ${p_j}^{sympto}$is the probability that an individual in age group $j$develops symptoms upon infection [21].

→ **Assuming a lower susceptibility of 0-19 y.o. compared to 20 y.o. and older**

Children have been suggested to be less susceptible to SARS-CoV-2 infection compared to adults, with younger children being less susceptible than teenagers. Uncertainty remains regarding the extent to which susceptibility increases with age. To further account for this uncertainty, we explore a scenario where children aged 0-9 y.o. are 50% less susceptible as those

20 y.o. and older and children aged 10-19 y.o. are 25% less susceptible than adults aged 20 y.o. and older [19].

For these three scenarios where we vary assumptions about infectivity and susceptibility by age, we derived adjusted contacts from the estimated effective contacts. We define adjusted contacts as the corresponding number of raw contacts assuming the difference in effective and raw contacts can be entirely explained by variations in susceptibility and infectivity in the different age groups. More specifically, let ${c_{i,j}}^{eff}$ denote the mean daily number of effective contacts that an individual aged i has with individuals aged j. Let σ_i (respectively θ_i) denote the susceptibility (respectively the infectivity) of age group i. The adjusted mean daily number of contacts is then derived as:

$$ {c_{i,j}}^{adj} = \frac{{c_{i,j}}^{eff}}{\sigma_i \cdot \theta_j} $$

→ **Including the population of elderly homes in the study population**

Since the beginning of the pandemic, elderly homes have accounted for a substantial share of the number of COVID-19 deaths in France [31]. As the epidemic dynamics in these locations as well as the structure of contacts is expected to be significantly different than that in the community, we removed the population of elderly homes from the French population for our baseline scenario and we discarded the results of tests from elderly homes residents. The SI-VIC surveillance system does not distinguish from all patients admitted in hospitals following a SARS-CoV-2 infection, those that live in elderly homes. In our baseline scenario, we removed the population of elderly homes from the study population and from the test data used for the calibration. As an indeterminate fraction of hospitalizations reported in the SI-VIC database are likely to be attributable to elderly home residents, we conduct a sensitivity analysis keeping the population of elderly homes in our study population and keeping using the tests results from elderly home patients for our calibration. The choice of this baseline scenario where we removed elderly homes population was motivated by the low share of elderly residents among all individuals admitted to hospital (6.5% from 1 March 2020 to 21 February 2021 ; 11.1% of the 70 y.o. and older assuming all admitted residents are 70 y.o. and older)..

→ **Considering quadratic reductions in contact patterns**

In our baseline scenario, we considered linear reduction in contact patterns. For instance, regarding the simulation of strategies targeting different age groups, this meant that when we were considering a reduction of 10% among 20-29 y.o., the contacts of this age group with all other age groups were reduced by 10%. With the same notation as the one used in the methods section, we used the following model:

$$ C^{interv} = ({c_{i,j}}^{interv}) = (min({\alpha_i}^{interv}, {\alpha_j}^{interv}) \cdot {c_{i,j}}^{eff}) $$

An alternative to model the impact of different reductions in contact patterns is to consider quadratic reduction in contact patterns. In this case, a reduction of 10% in mobility among 20-29 y.o. would correspond to a 10% reduction in contact between 20-29 y.o. and all other age groups

and a reduction of 19% of contacts of 20-29 y.o. with 20-29 y.o. compared to the equation detailed above, we use the following parametrization:
$C^{interv} = ({c_{i,j}}^{interv}) = ({\alpha_i}^{interv} \cdot {\alpha_j}^{interv} \cdot {c_{i,j}}^{eff})$

→ **Assuming contact patterns are only modified outside the household**

In our baseline scenario, we assumed that when an age group reduces their contacts, this affects the contacts of all other age groups homogeneously. Non-pharmaceutical interventions implemented have mostly been targeting contacts outside the household, so that this assumption might not hold for household contacts. Studies have for instance reported that, when interventions were implemented, contacts between school-aged children were removed whereas some contacts with younger adults were maintained (e.g. with parents)[58] . We explore a sensitivity analysis where only contacts outside the household are modified following the same approach as in our baseline scenario (homogeneous reduction outside the household).

Supplementary text

The abbreviations used for the names of the metropolitan French regions are:

ARA: Auvergne-Rhônes-Alpes
BFC: Bourgogne-Franche-Comté
BRE: Bretagne
CVL: Centre Val de Loire
COR: Corse
GES: Grand Est
HDF: Hauts-de-France
IDF: Île-de-France
NAQ: Nouvelle-Aquitaine
NOR: Normandie
OCC: Occitanie
PAC: Provence Alpes Côte d'Azur
PDL: Pays de la Loire

Supplementary materials

Figure S1

Figure S1: Map of the 13 regions of metropolitan France

Figure S2

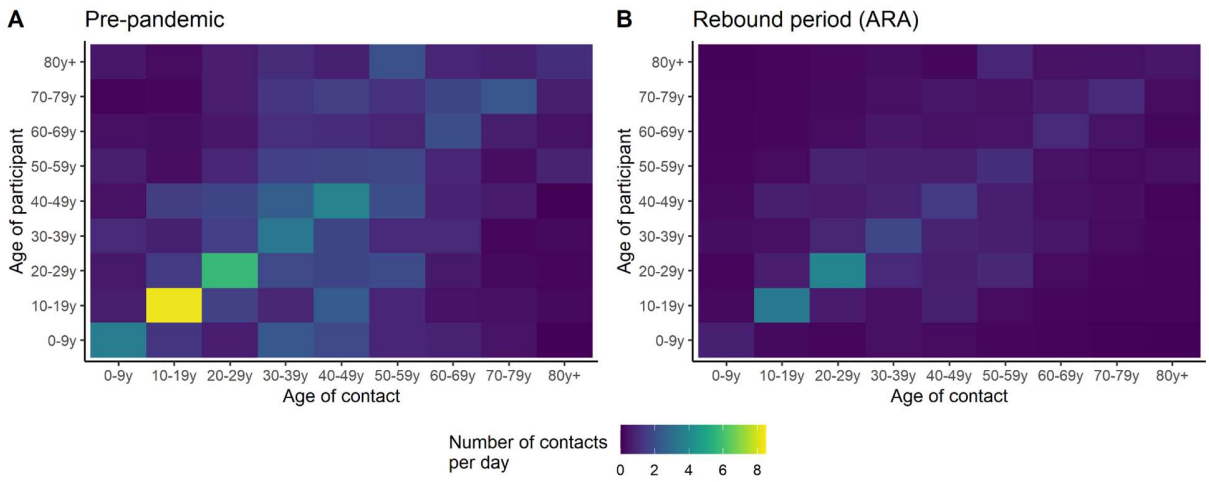

Figure S2: Contact matrices across different periods. (A) Contact matrix describing the mixing patterns during the pre-pandemic era [41]. **(B)** Effective contact matrix describing the mixing patterns between July 9th, 2020 and September 28th, 2020 in the Auvergne-Rhône-Alpes region.

Figure S3

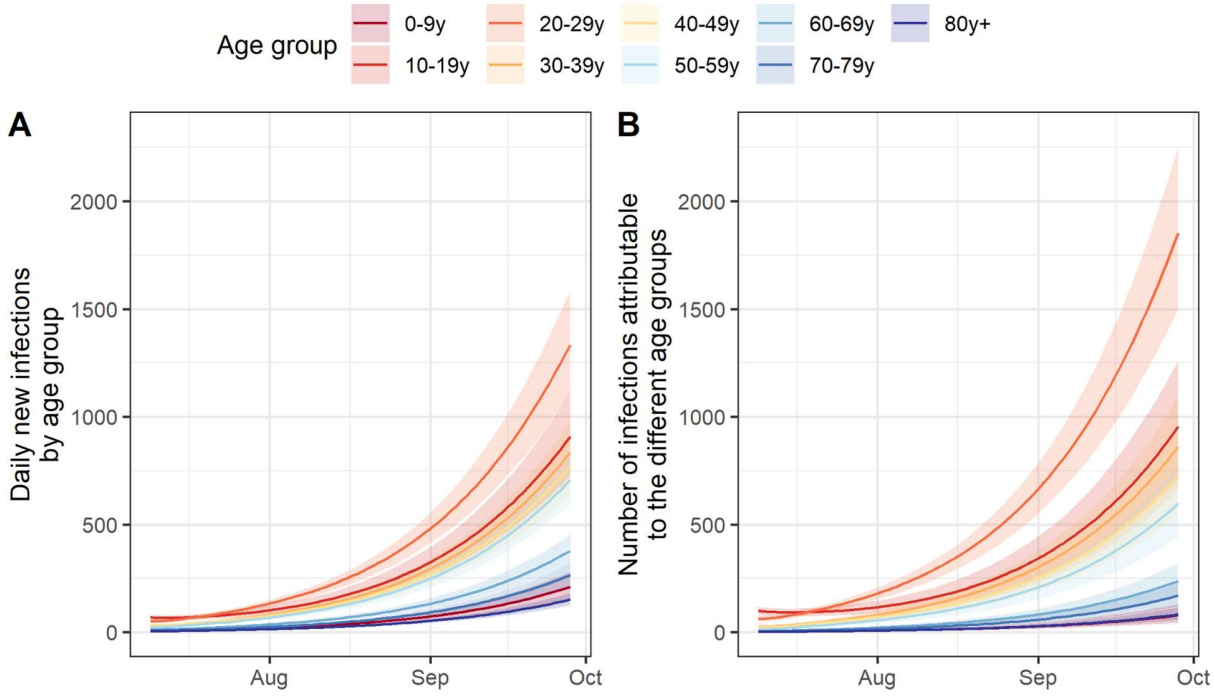

Figure S3: Dynamics of infections in the different age groups. (A) Daily new infections by age group. **(B)** Number of daily new infections attributable to the different age groups. The results are reported for the Auvergne-Rhône-Alpes region during the rebound period (9 July-28 September 2020). The shaded areas correspond to 95% credible intervals.

Figure S4

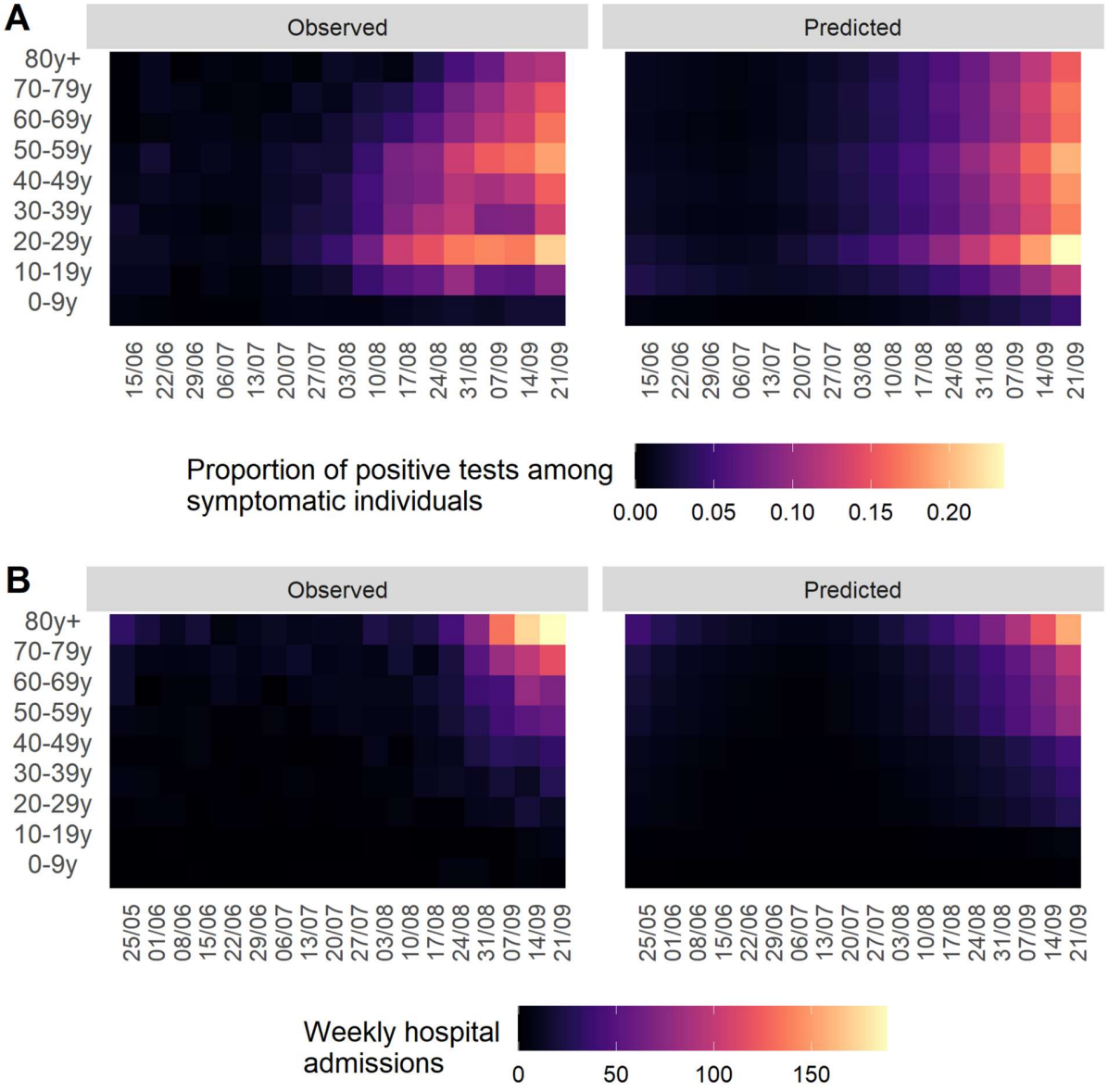

Figure S4: Predicted and observed dynamics of the epidemic in Auvergne-Rhône-Alpes across age-groups. (A) Observed and predicted dynamics of the proportion of positive tests among symptomatic individuals tested by age-group. **(B)** Observed and predicted dynamics of the weekly hospital admissions by age-group.

Figure S5

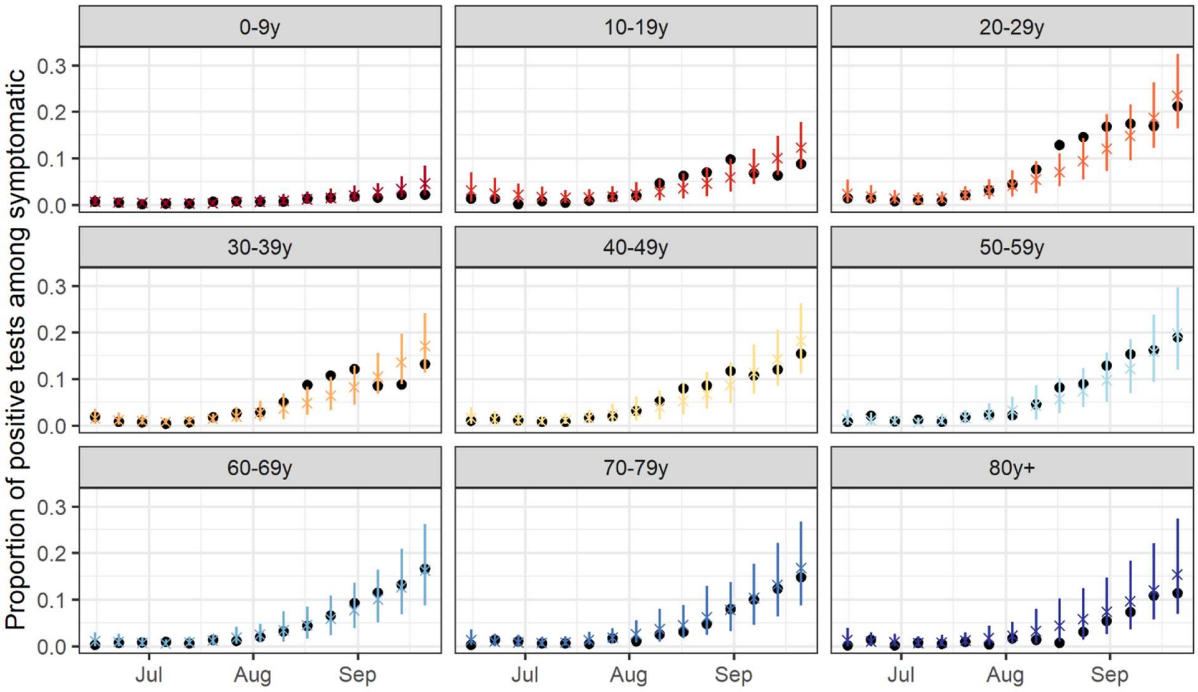

Figure S5: Model-predicted and observed proportion of positive tests among symptomatic individuals in Auvergne-Rhône-Alpes by age group. Proportion of positive test among symptomatic individuals aged 0-9 y.o., 10-19 y.o., 20-29 y.o., 30-39 y.o., 40-49 y.o., 50-59 y.o., 60-69 y.o., 70-79 y.o. And over 80 y.o. in Auvergne-Rhône-Alpes. The colored crosses indicate model predictions. The black points indicate the proportions of positive tests among symptomatic individuals extracted from the SIDEP database.

Figure S6

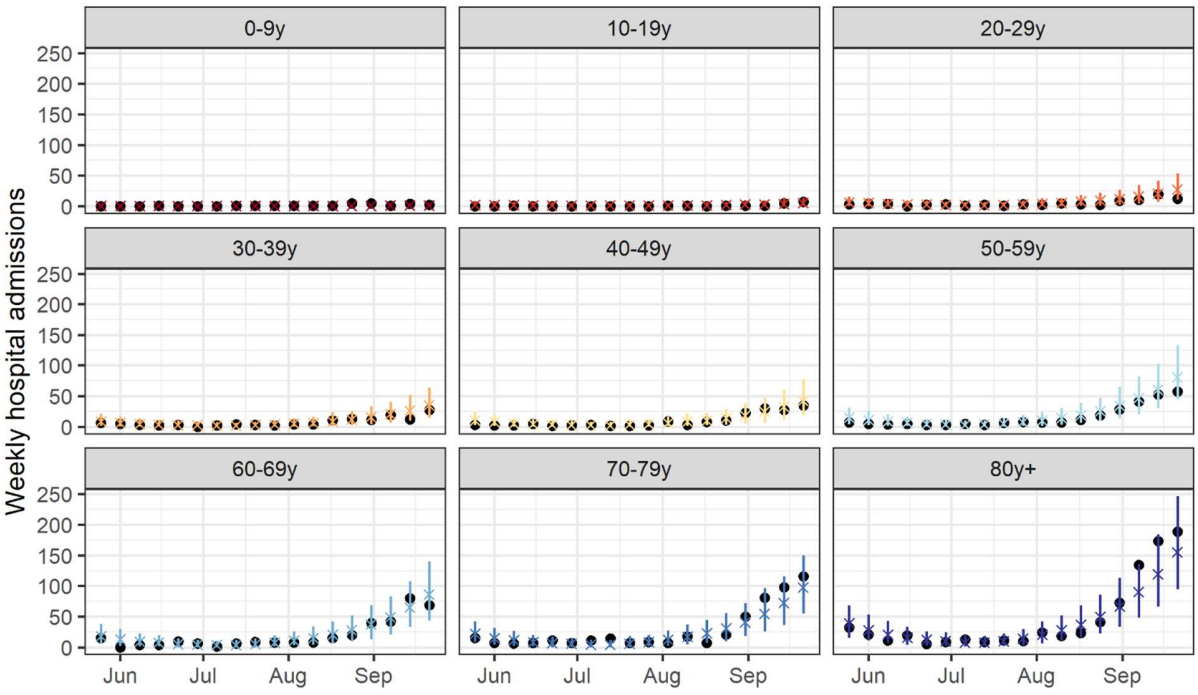

Figure S6: Model predicted and observed age-stratified hospital admissions in Auvergne-Rhône-Alpes by age group. Weekly hospital admissions of individuals aged 0-9 y.o., 10-19 y.o., 20-29 y.o., 30-39 y.o., 40-49 y.o., 50-59 y.o., 60-69 y.o., 70-79 y.o. and over 80 y.o. in Auvergne-Rhône-Alpes. The colored crosses and segments indicate model predictions. The black points indicate weekly hospital admissions extracted from the SI-VIC database.

Figure S7

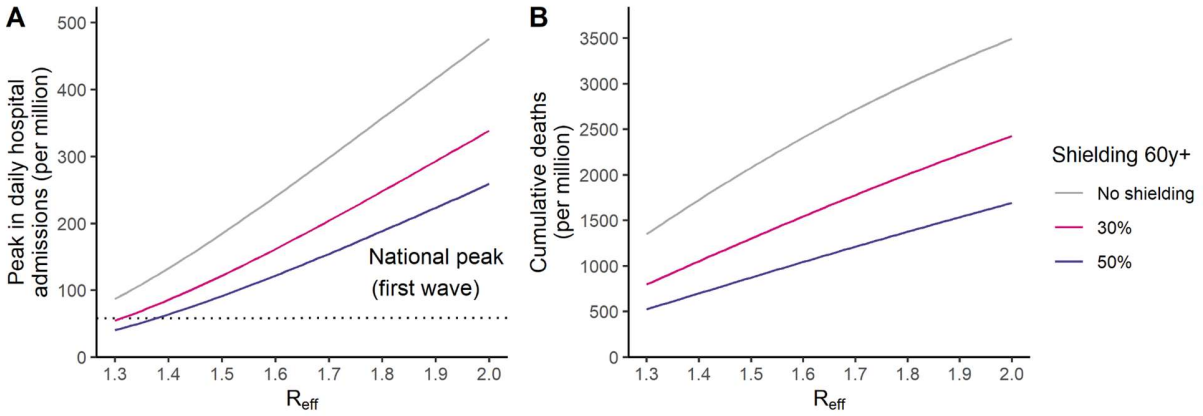

Figure S7: Impact of strategies shielding those aged 60 y.o. and above. (A) Peak in hospital admissions per million and **(B)** number of deaths per million as a function of the effective reproduction number R_{eff} assuming a reduction of 50% or 30% in effective contacts of those older than 60 y.o. The number of deaths is computed from the time interventions are implemented until the end of the simulation.

Figure S8

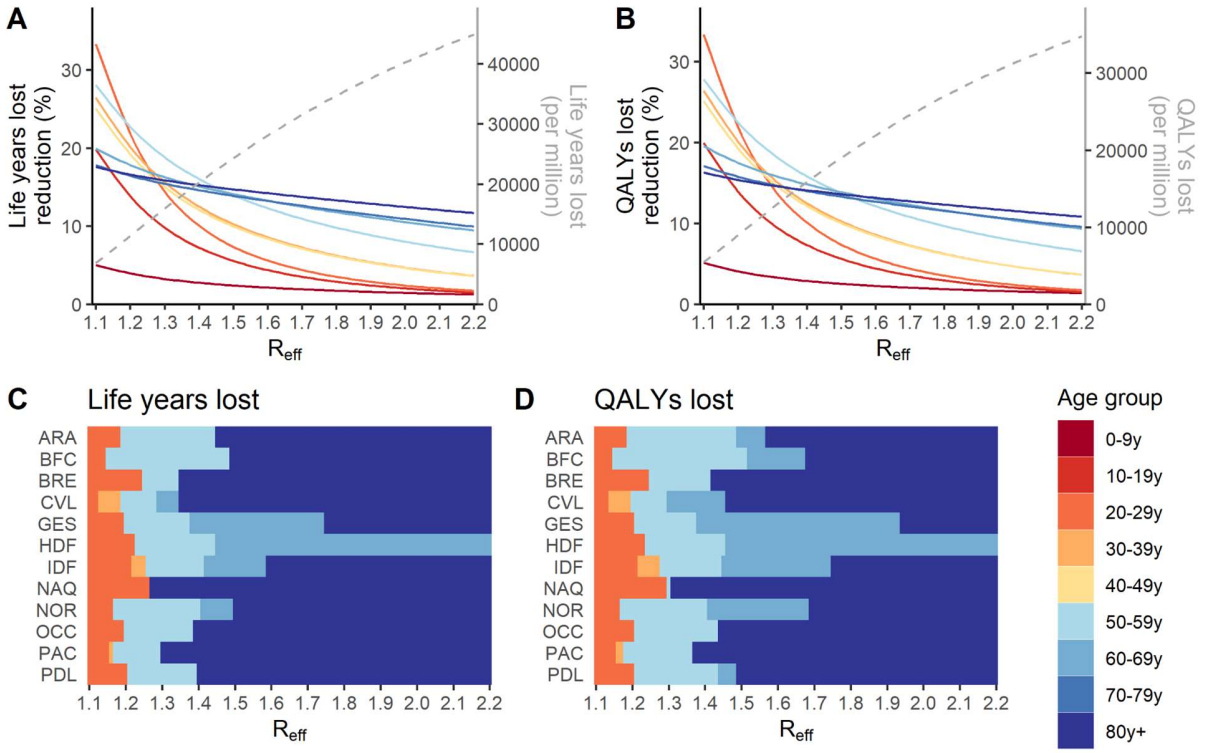

Figure S8: Impact of strategies targeting specific age groups on the number of life-years lost. Reduction in **(A)** the number of life-years lost and **(B)** the number of QALYs lost in Auvergne-Rhône-Alpes region as a function of the effective reproduction number R_{eff} when the intervention is implemented for a reduction of 1 contact. The grey dotted lines indicate, in the absence of additional measure, the value of the target metrics. Age-groups for which a reduction of 1 contact results in the highest impact on the reduction of **(C)** the number of life years lost and **(D)** the number of QALYs lost as a function of the effective reproduction number R_{eff}. Region's abbreviations are detailed in supplementary text.

Figure S9

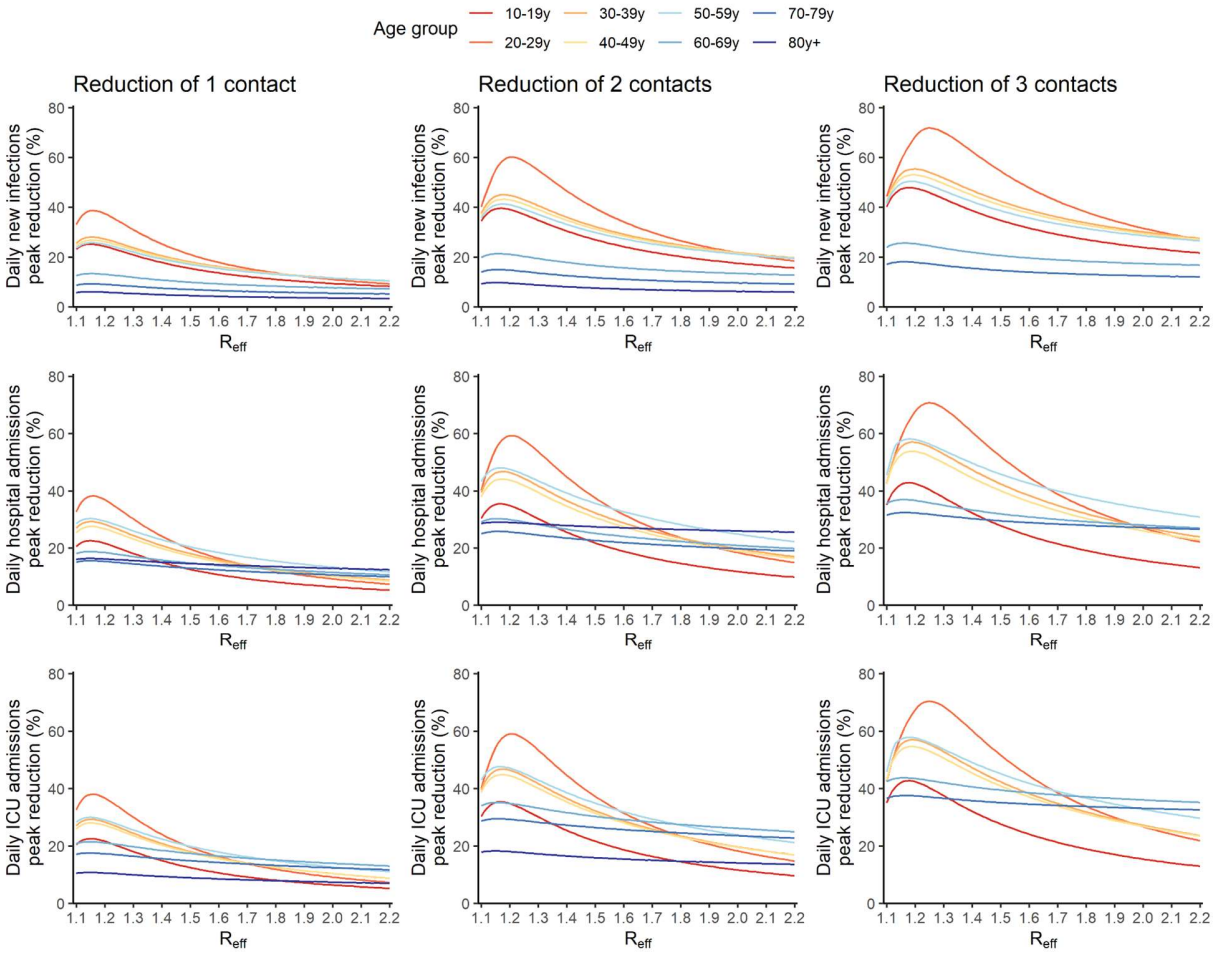

Figure S9: Impact of larger reduction of contacts for strategies targeting different age groups in Auvergne-Rhône-Alpes on the peak in daily new infections (first line), the peak in hospital admissions (second line) and the peak in daily ICU admissions (third line) as a function of the effective reproduction number R_{eff} when the intervention is implemented. Results are displayed for a reduction of 1 contact (first column), 2 contacts (second column) and 3 contacts (third column) in the targeted age groups.

Figure S10

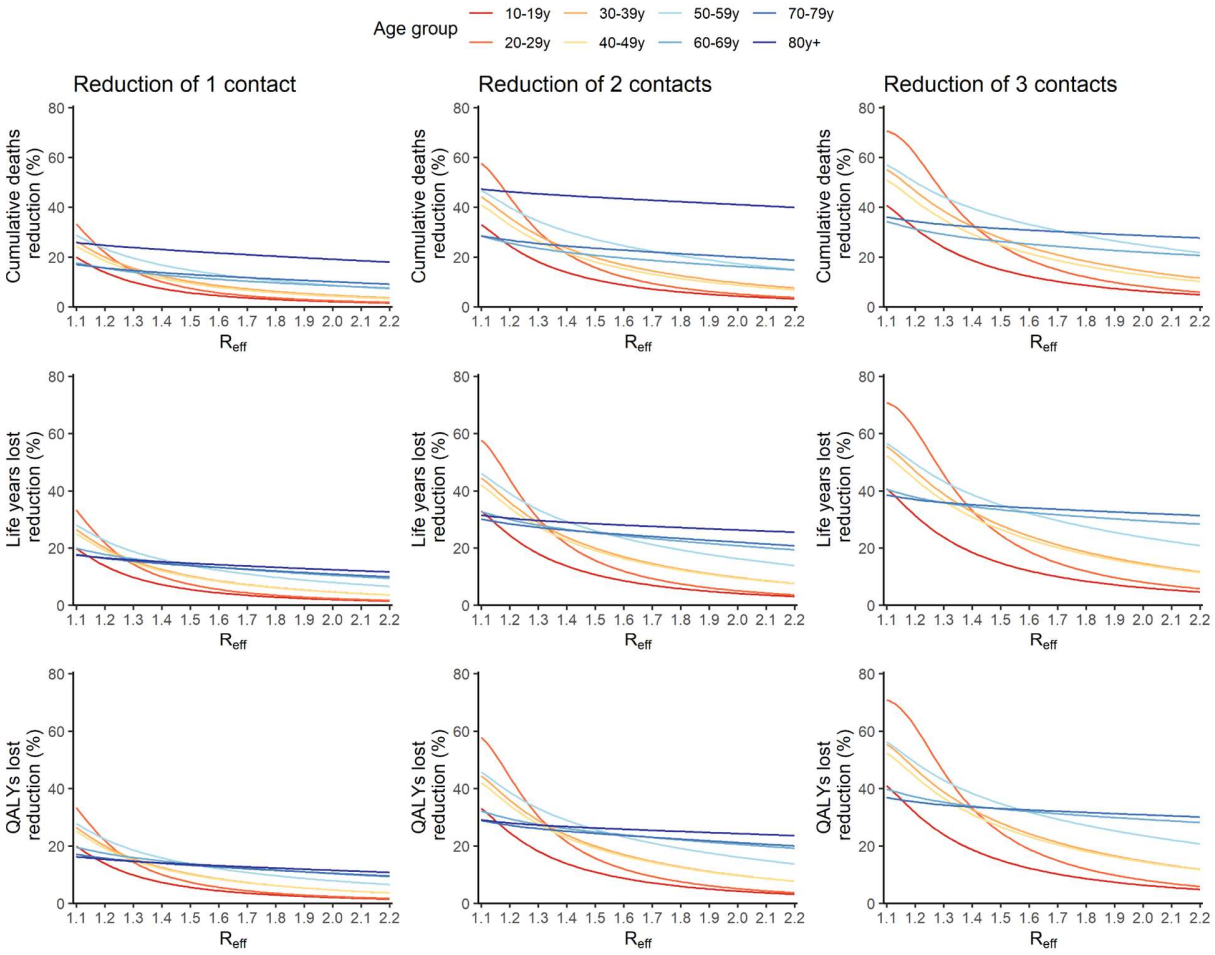

Figure S10: Impact of larger reduction of contacts for strategies targeting different age groups in Auvergne-Rhône-Alpes on the number of deaths (first line), life years lost (second line) and QALYs lost (third line) after the implementation of the intervention as a function of the effective reproduction number R_{eff} when the intervention is implemented.

Figure S11

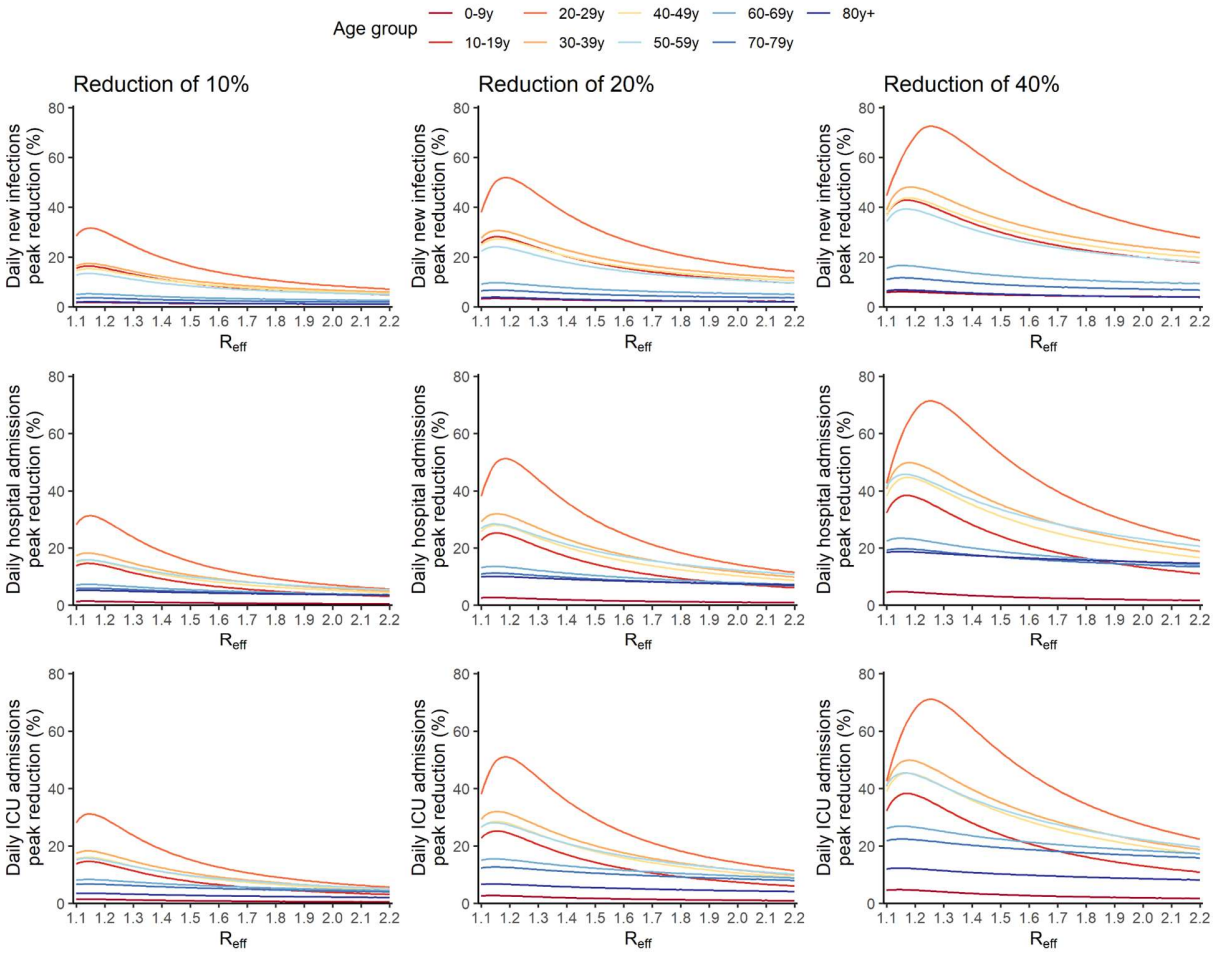

Figure S11: Impact of strategies targeting different age groups in Auvergne-Rhône-Alpes on the peak in daily new infections (first line), the peak in hospital admissions (second line) and the peak in daily ICU admissions (third line) as a function of the effective reproduction number R_{eff} when the intervention is implemented. Results are displayed for a reduction of 10% (first column), 20% (second column) and 40% (third column) in the number of contacts of the targeted age groups.

Figure S12

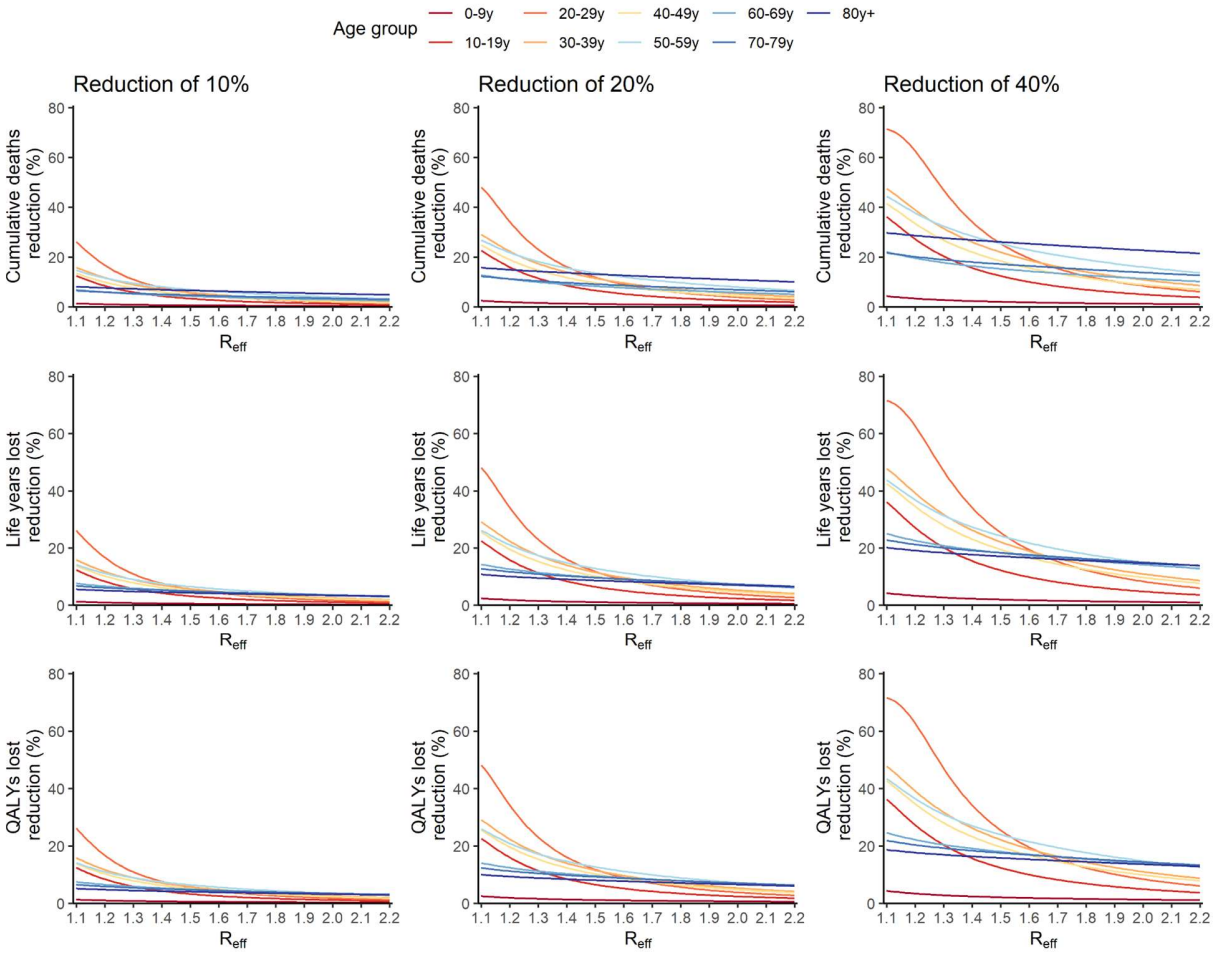

Figure S12: Impact of strategies targeting different age groups in Auvergne-Rhône-Alpes on the number of deaths (first line), the life years lost (second line) and the QALYs lost (third line) as a function of the effective reproduction number R_{eff} when the intervention is implemented. Results are displayed for a reduction of 10% (first column), 20% (second column) and 40% (third column) in the number of contacts of the targeted age groups.

Figure S13

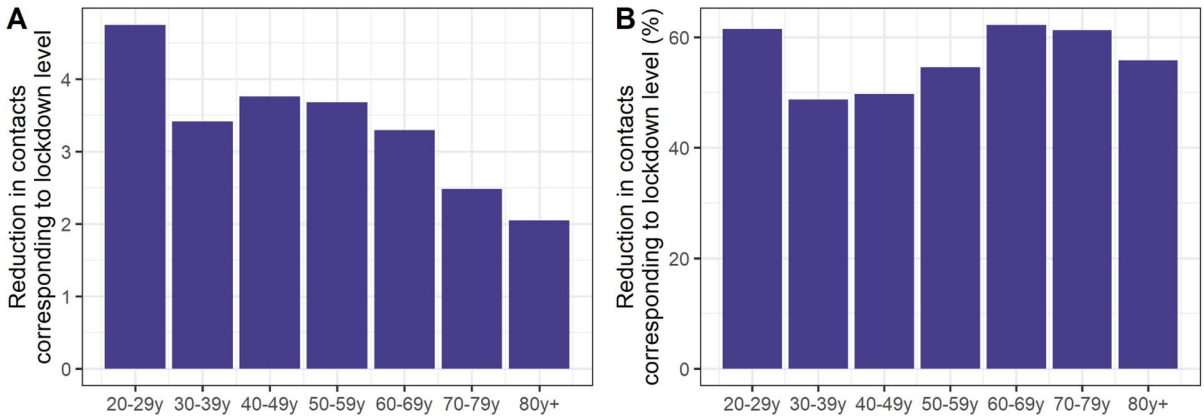

Figure S13: Reduction in contacts necessary to move the number of contacts from levels measured during summer 2020 to those measured during the first lockdown of spring 2020. Results are reported both in absolute (A) and (B) relative reductions. The reductions are computed using the contacts measured in the SocialCov survey during spring 2020 17 and summer 2020 (Table S2).

Legend for Figures S14-S25

(A) Proportion of positive tests among symptomatic individuals by age group. **(B)** Weekly hospital admissions of individuals by age group. The colored crosses and segments indicate model predictions. The colored crosses and segments indicate model predictions. The black points in panels (A) indicate the proportions of positive tests among symptomatic individuals extracted from the SIDEP database. The black points in panels (J-R) indicate weekly hospital admissions extracted from the SI-VIC database.

Figure S14: Model predictions and observations in Bourgogne-Franche-Comté

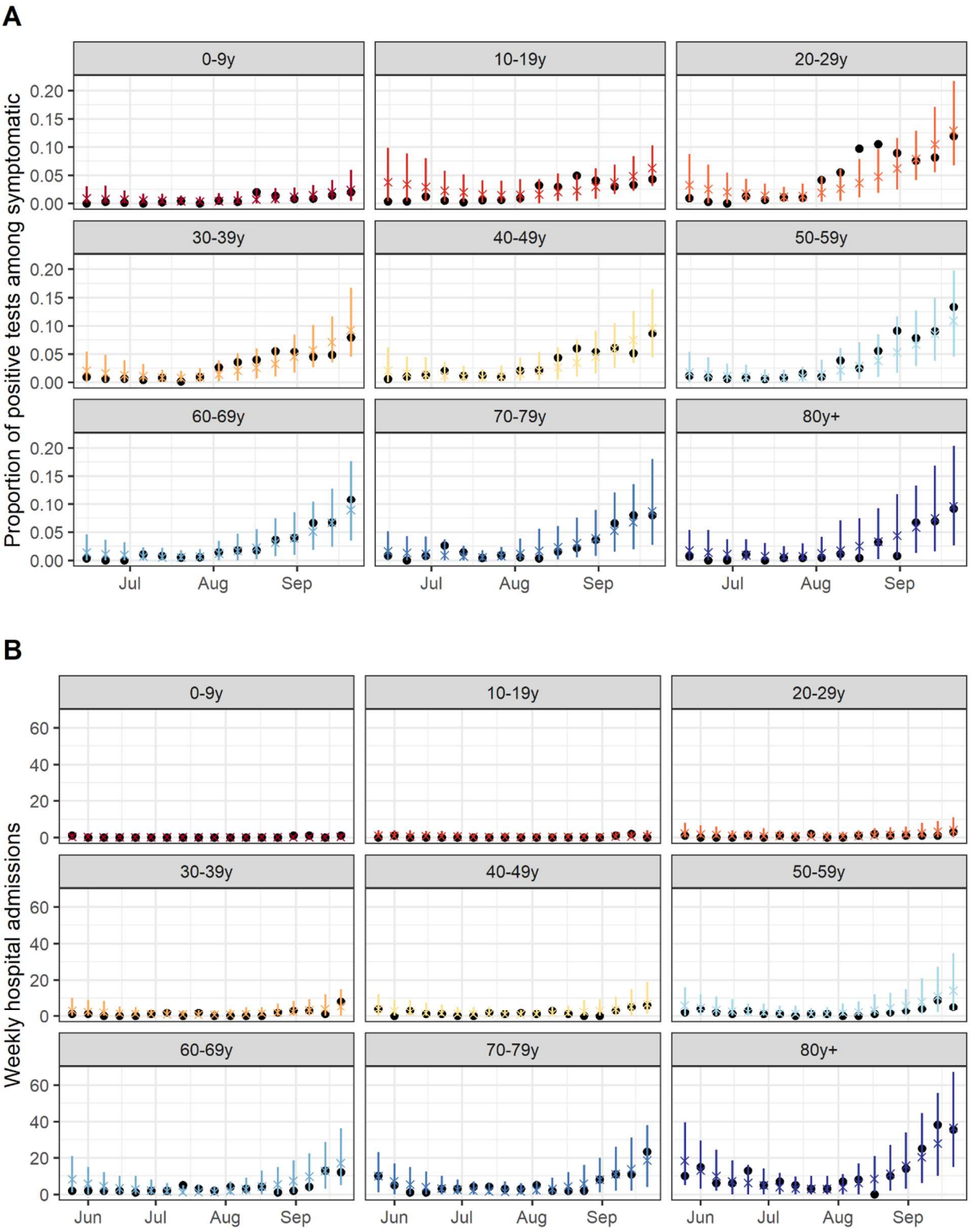

Figure S15: Model predictions and observations in the Bretagne region

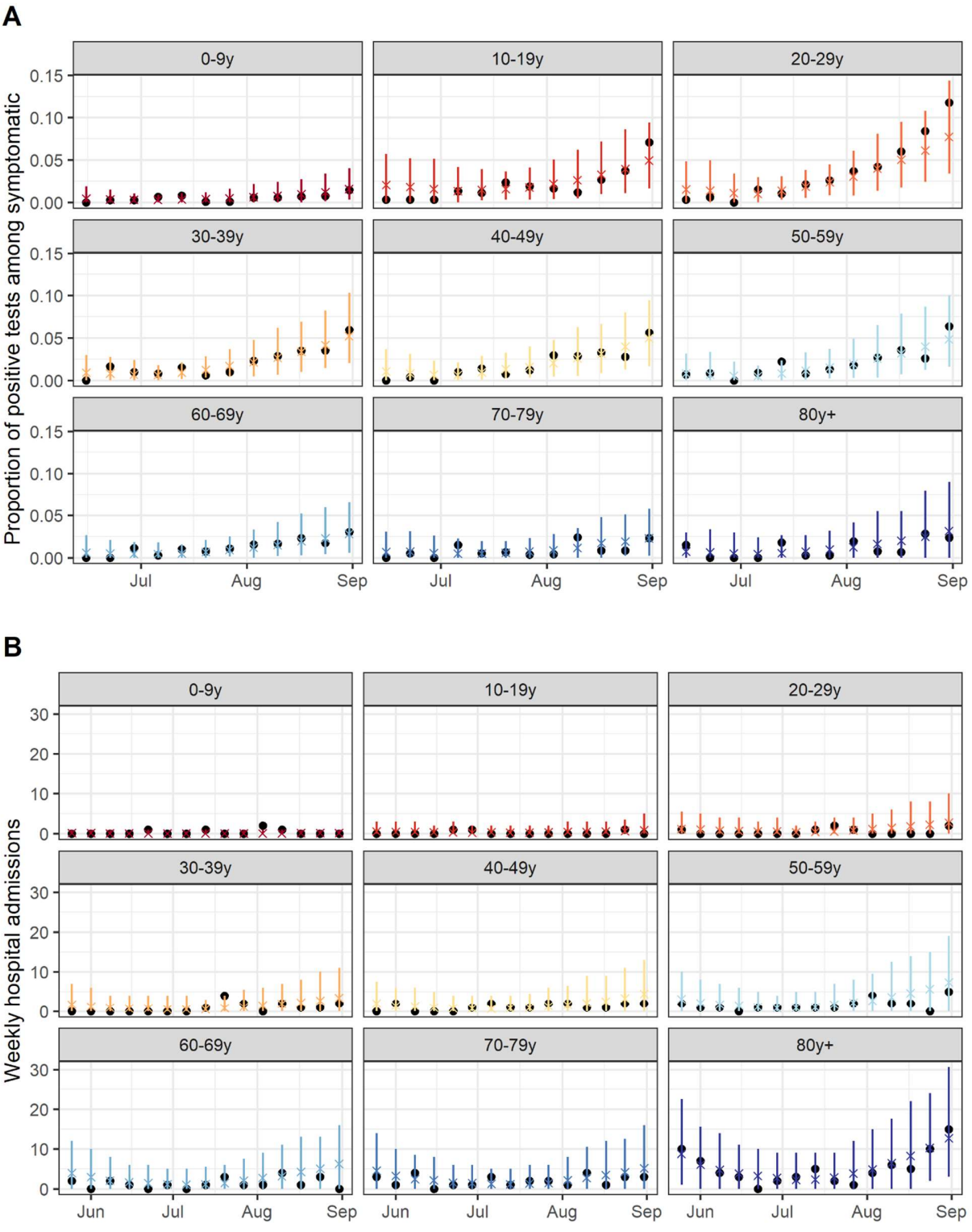

Figure S16: Model predictions and observations in the Centre-Val de Loire region

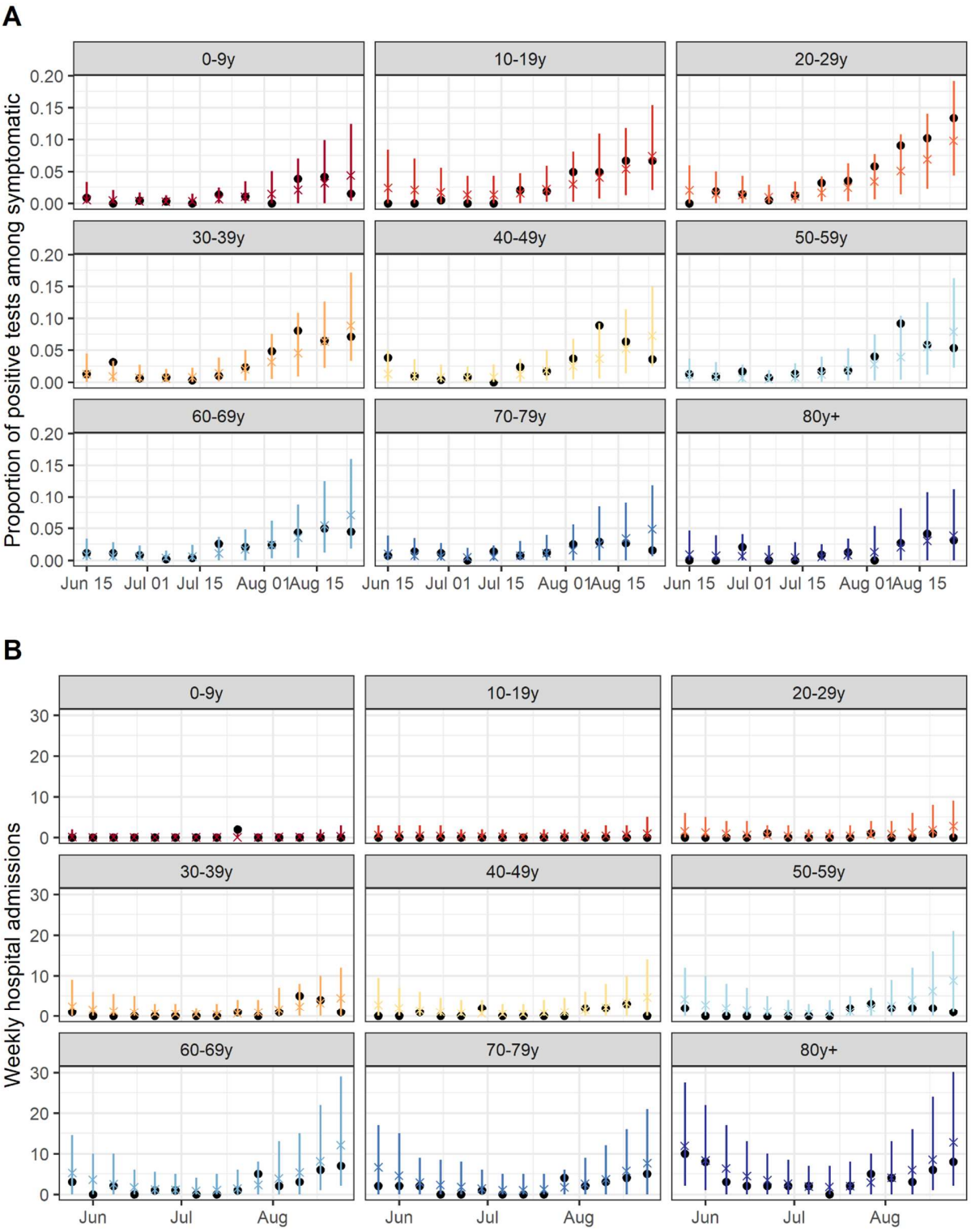

Figure S17: Model predictions and observations in the Corse region

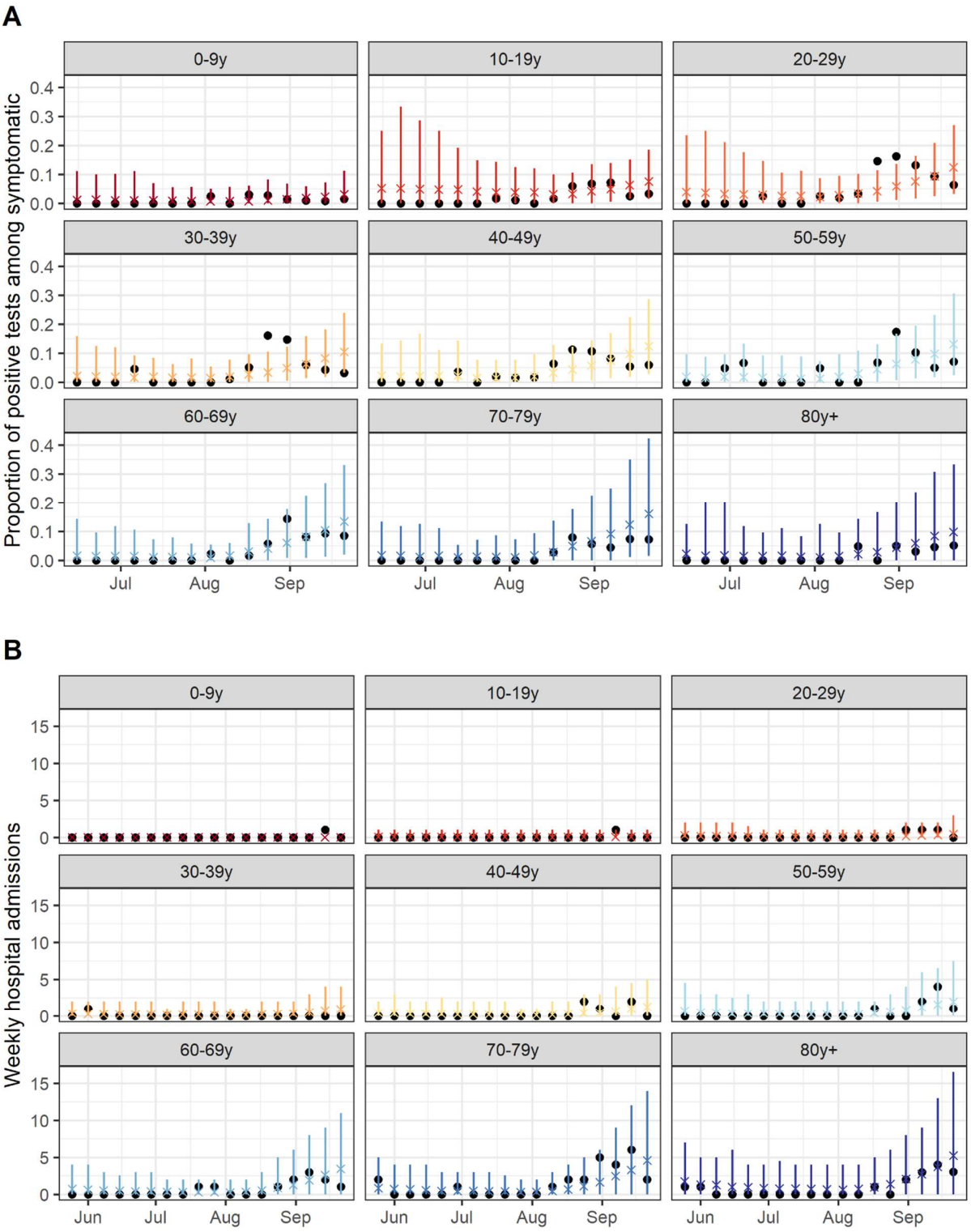

Figure S18: Model predictions and observations in the Grand Est region

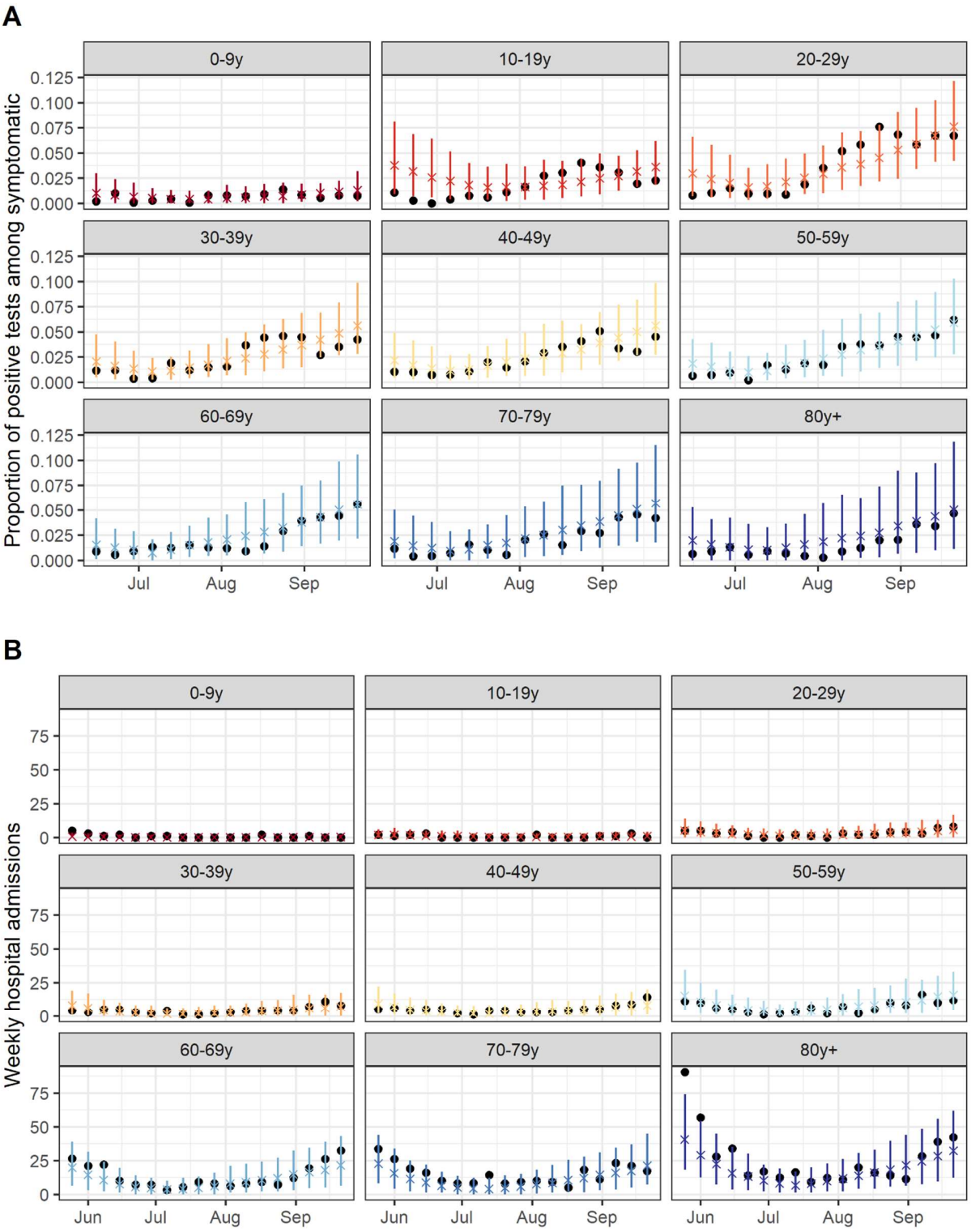

Figure S19: Model predictions and observations in the Hauts-de-France region

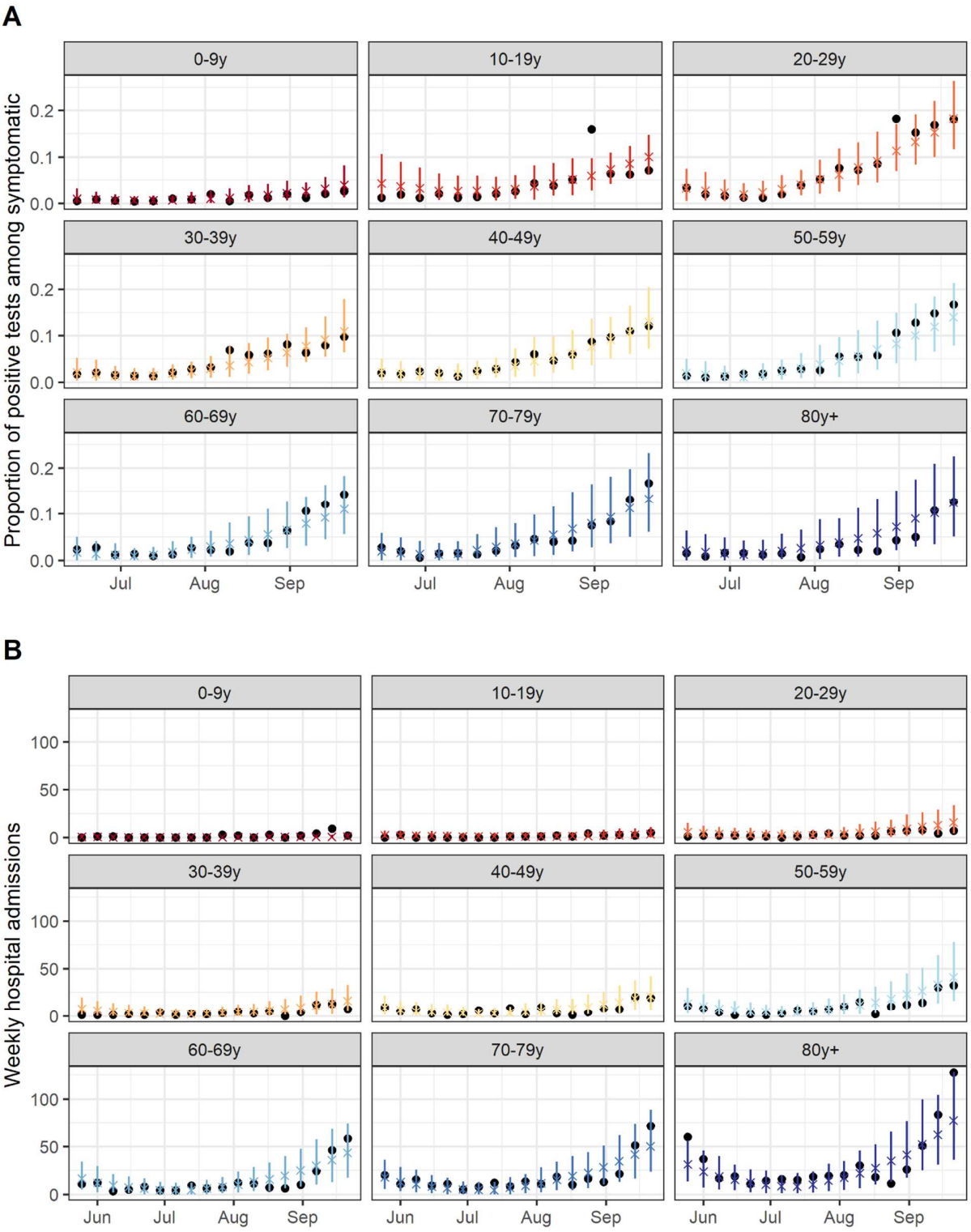

Figure S20: Model predictions and observations in the Île-de-France region

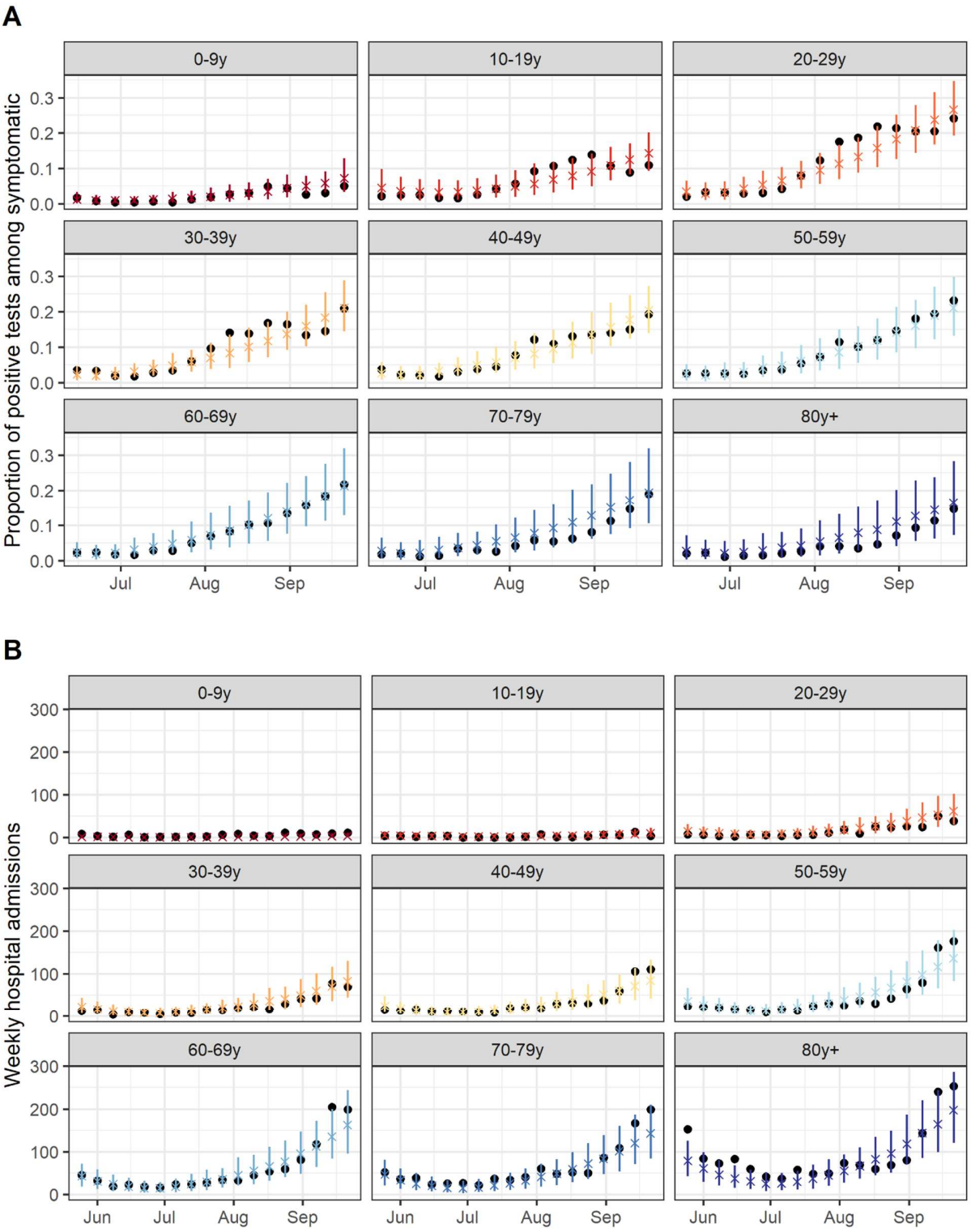

Figure S21: Model predictions and observations in the Nouvelle-Aquitaine region

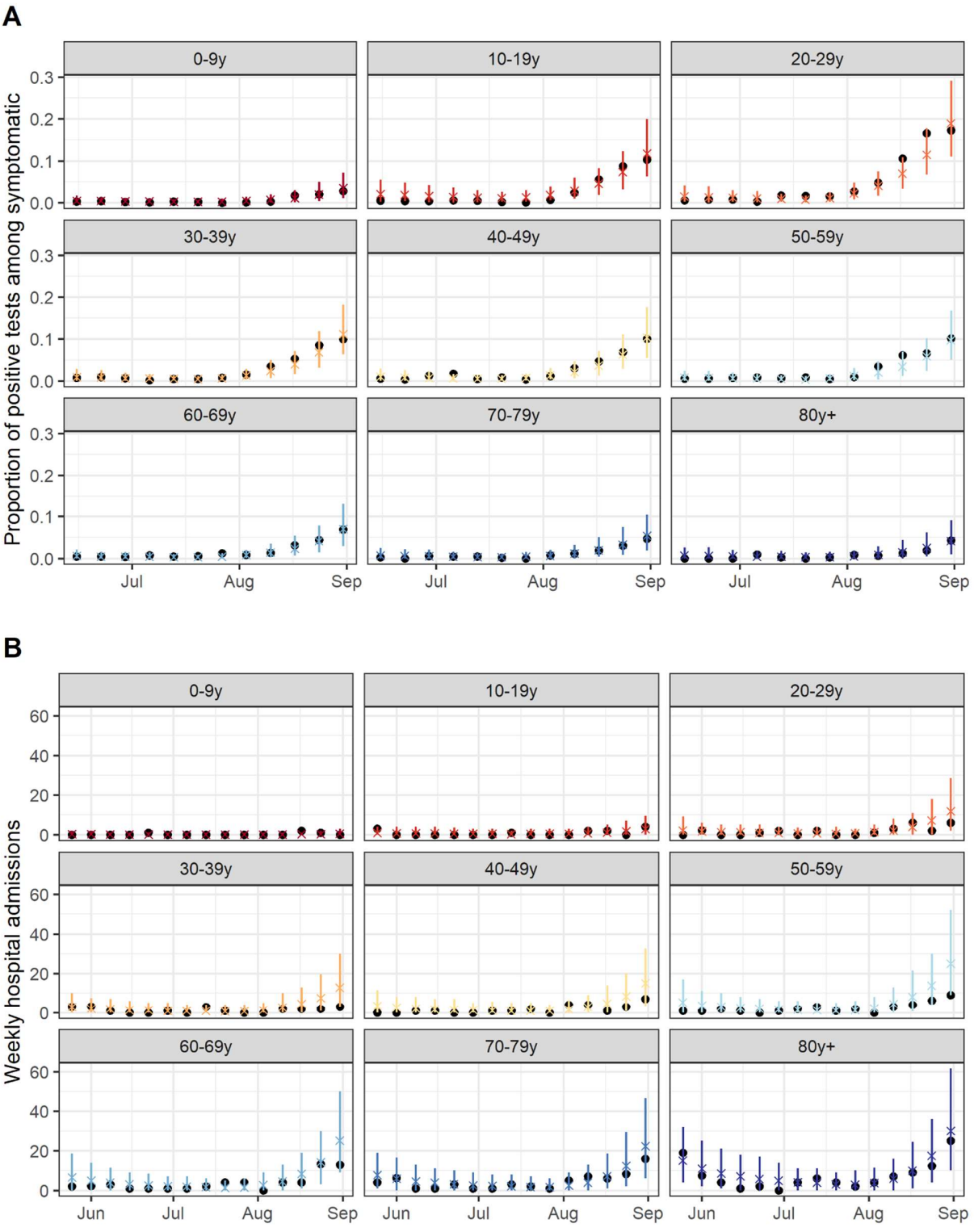

Figure S22: Model predictions and observations in the Normandie region

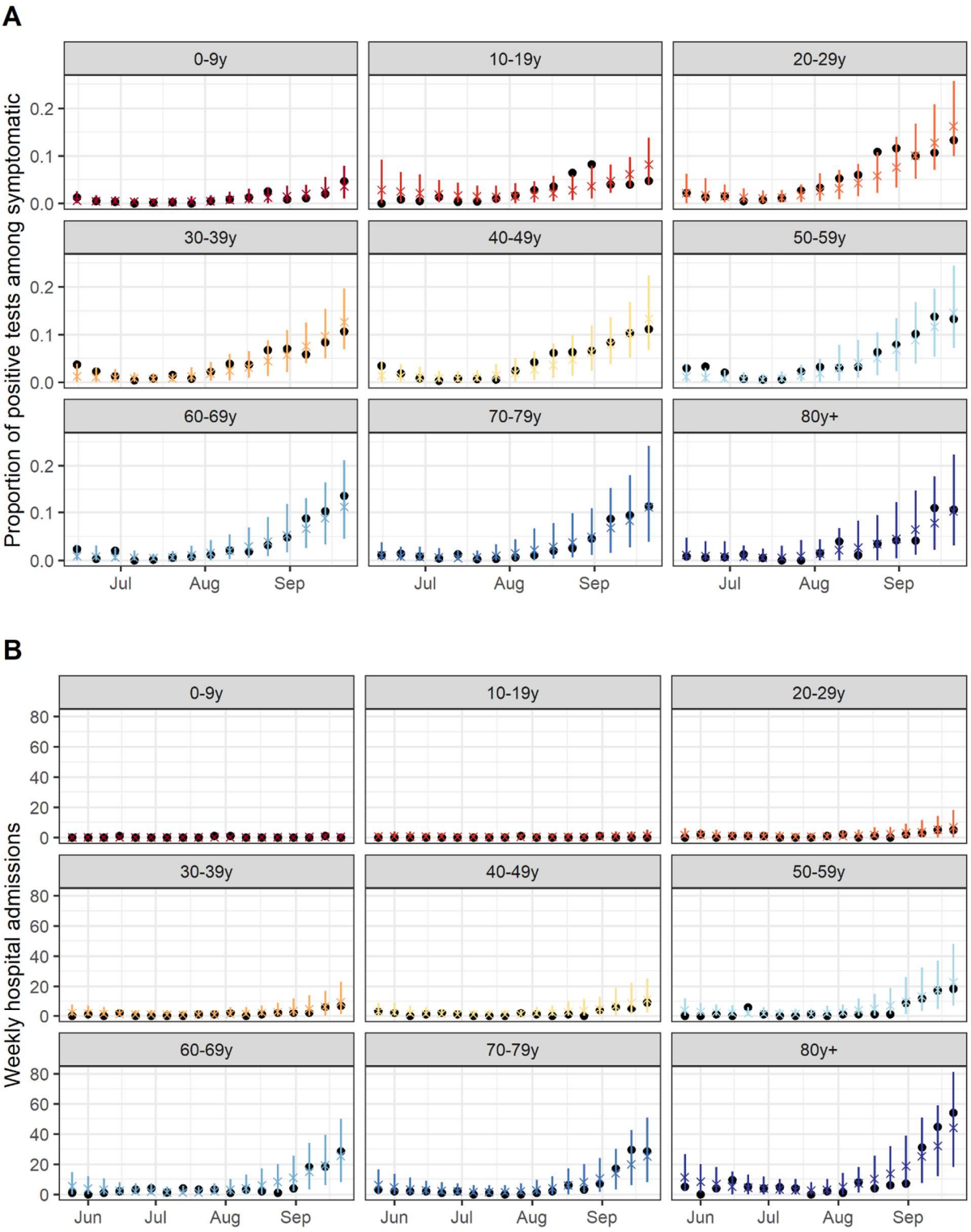

Figure S23: Model predictions and observations in the Occitanie region

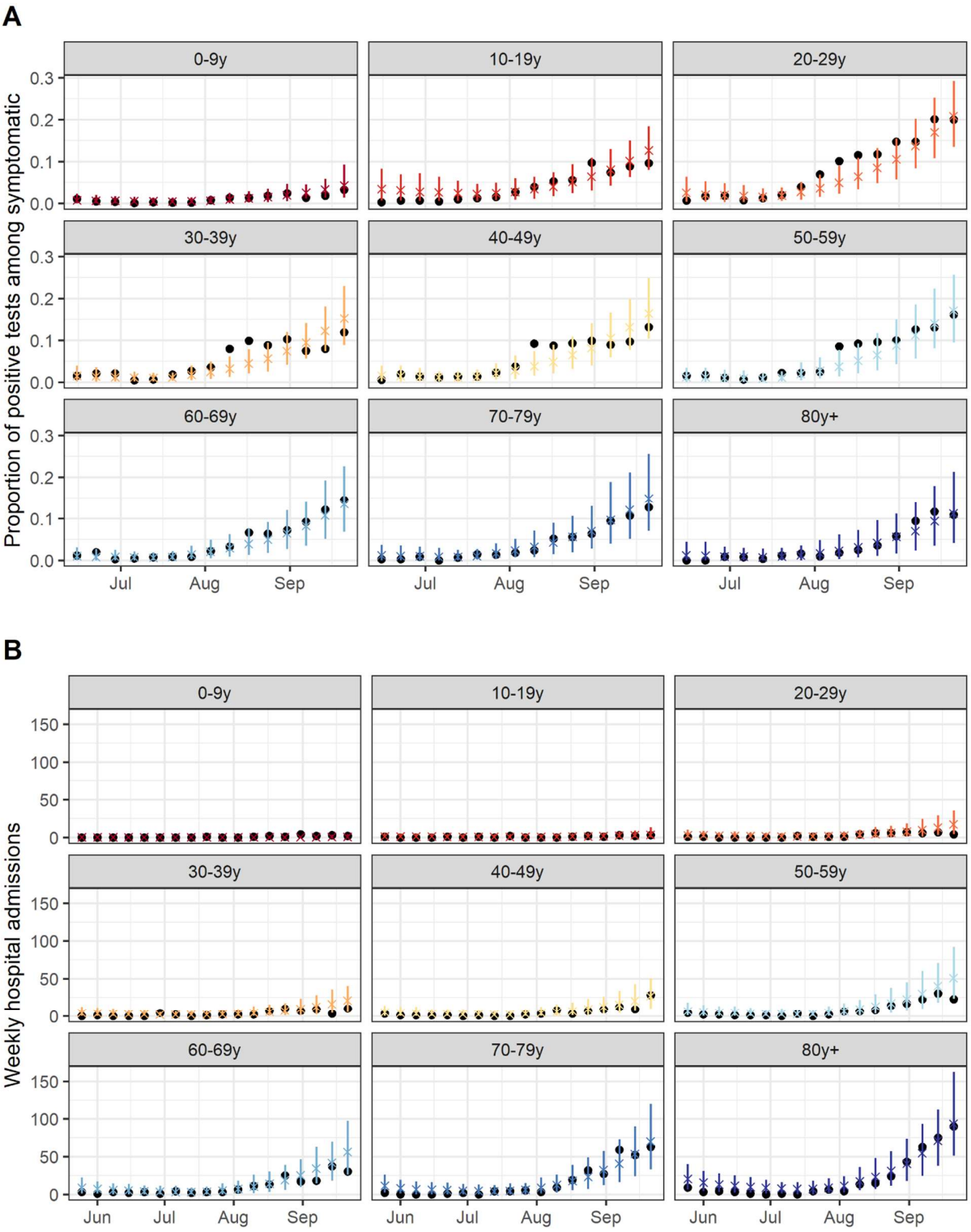

Figure S24: Model predictions and observations in Provence-Alpes Côte d'Azur

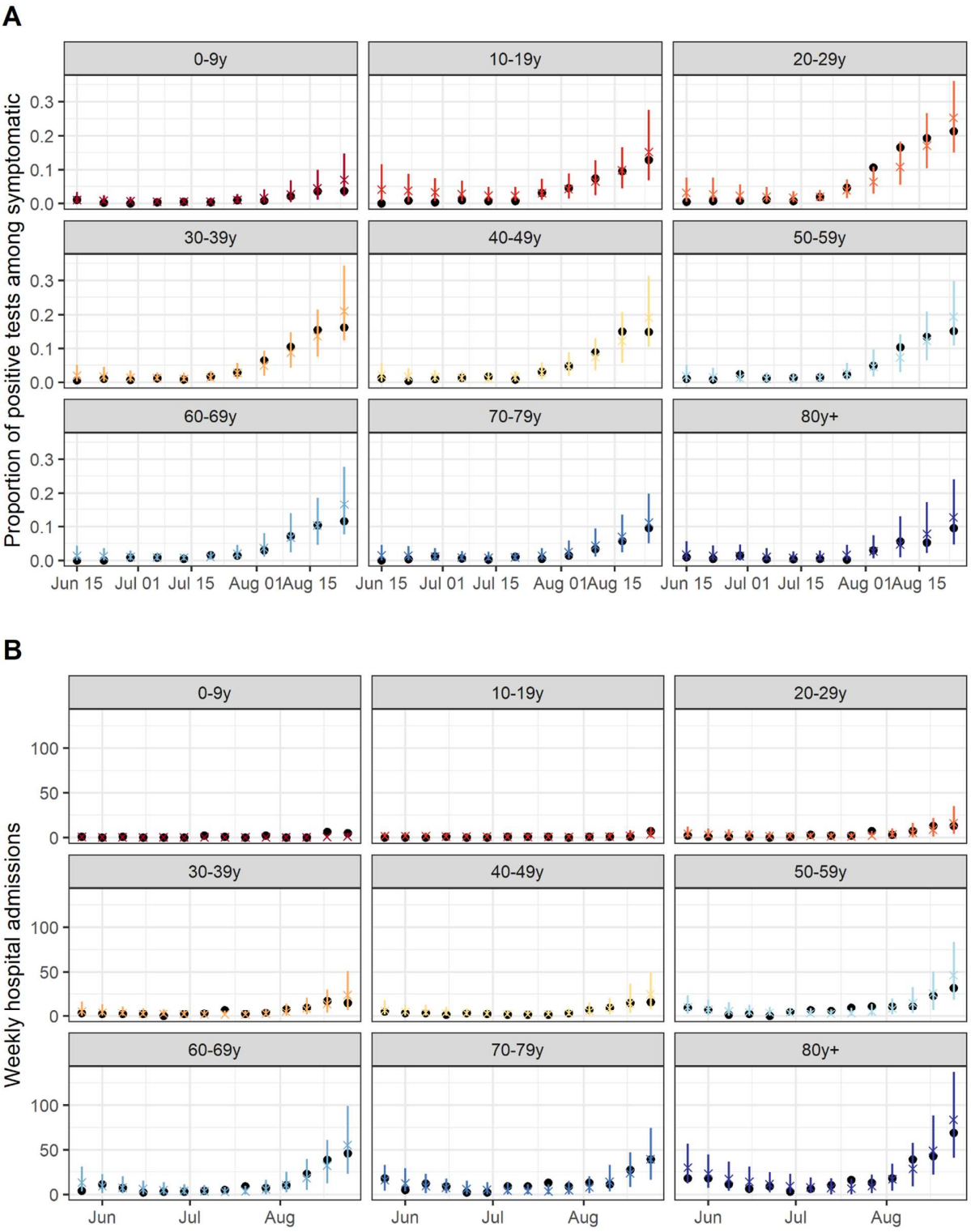

Figure S25: Model predictions and observations in the Pays de la Loire region

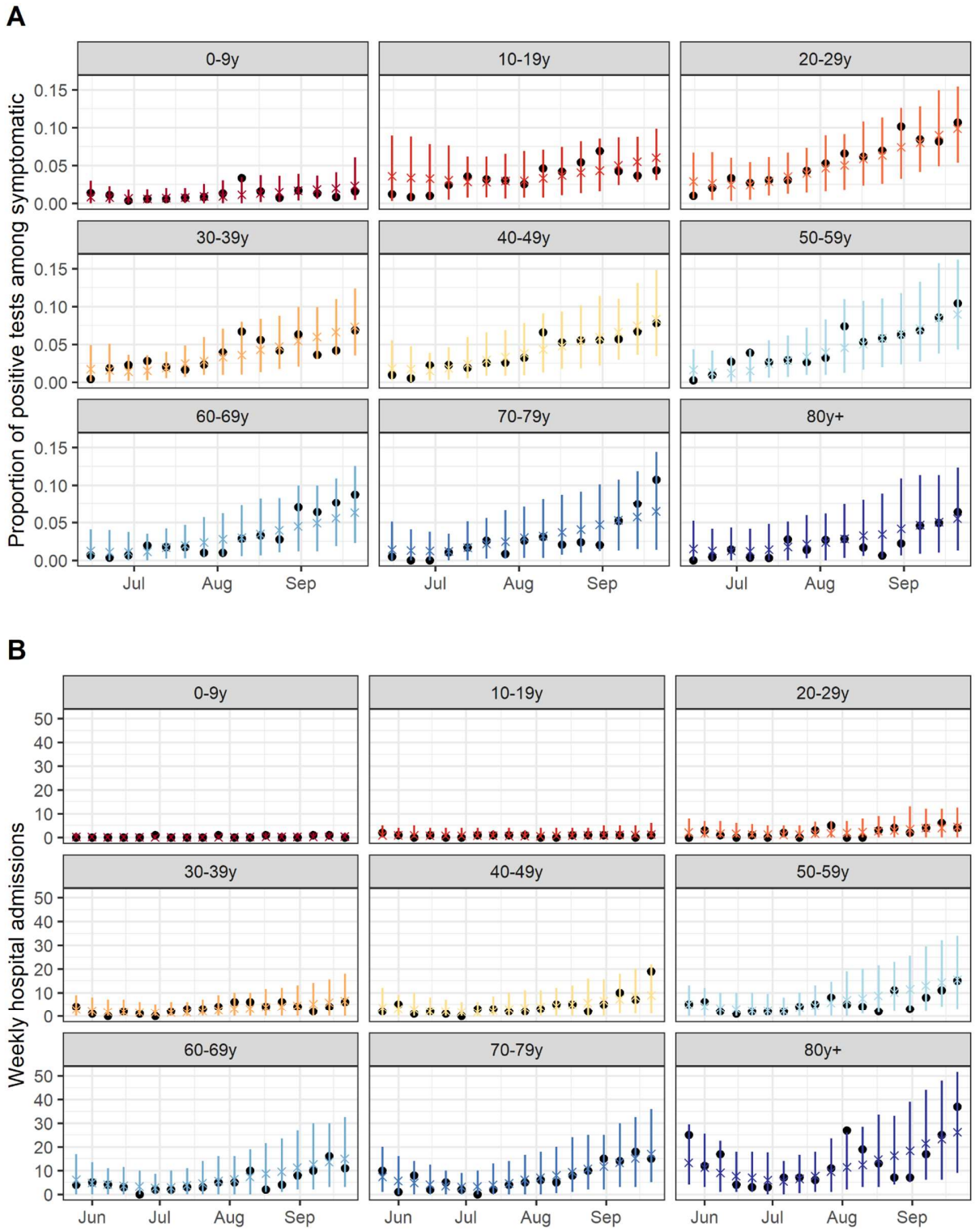

Figure S26

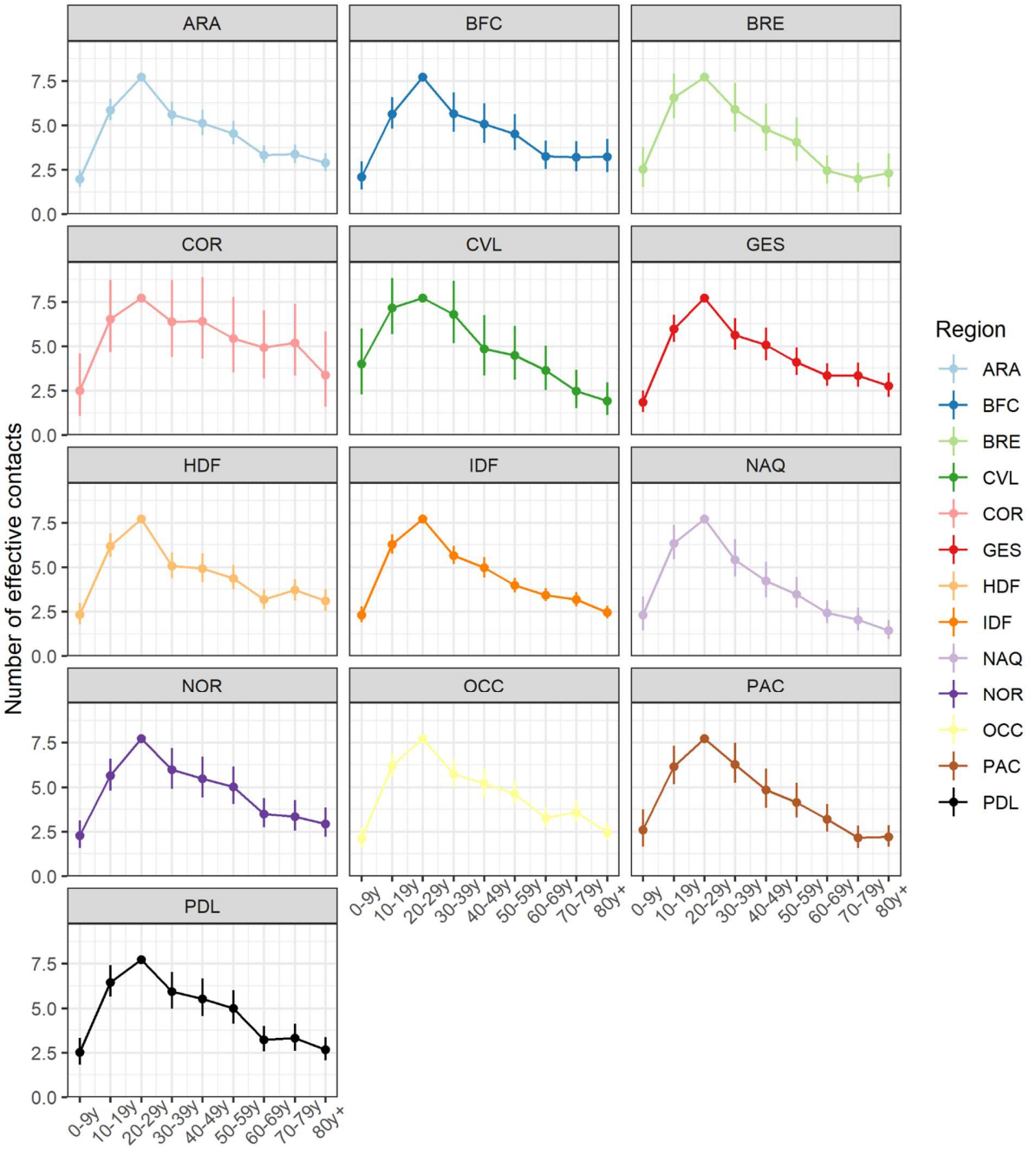

Figure S26: Estimates of the number of contacts during the rebound period in the 13 regions of Metropolitan France. Predicted number of effective contacts in the different age groups during the rebound period. ARA: Auvergne-Rhônes-Alpes ; BFC: Bourgogne-Franche-Comté ; BRE: Bretagne ; CVL: Centre Val de Loire ; COR: Corse ; GES: Grand Est ; HDF: Hauts-de-France; IDF: Île-de-France; NAQ: Nouvelle-Aquitaine; NOR: Normandie; OCC: Occitanie; PAC: Provence Alpes Côte d'Azur; PDL: Pays de la Loire

Figure S27

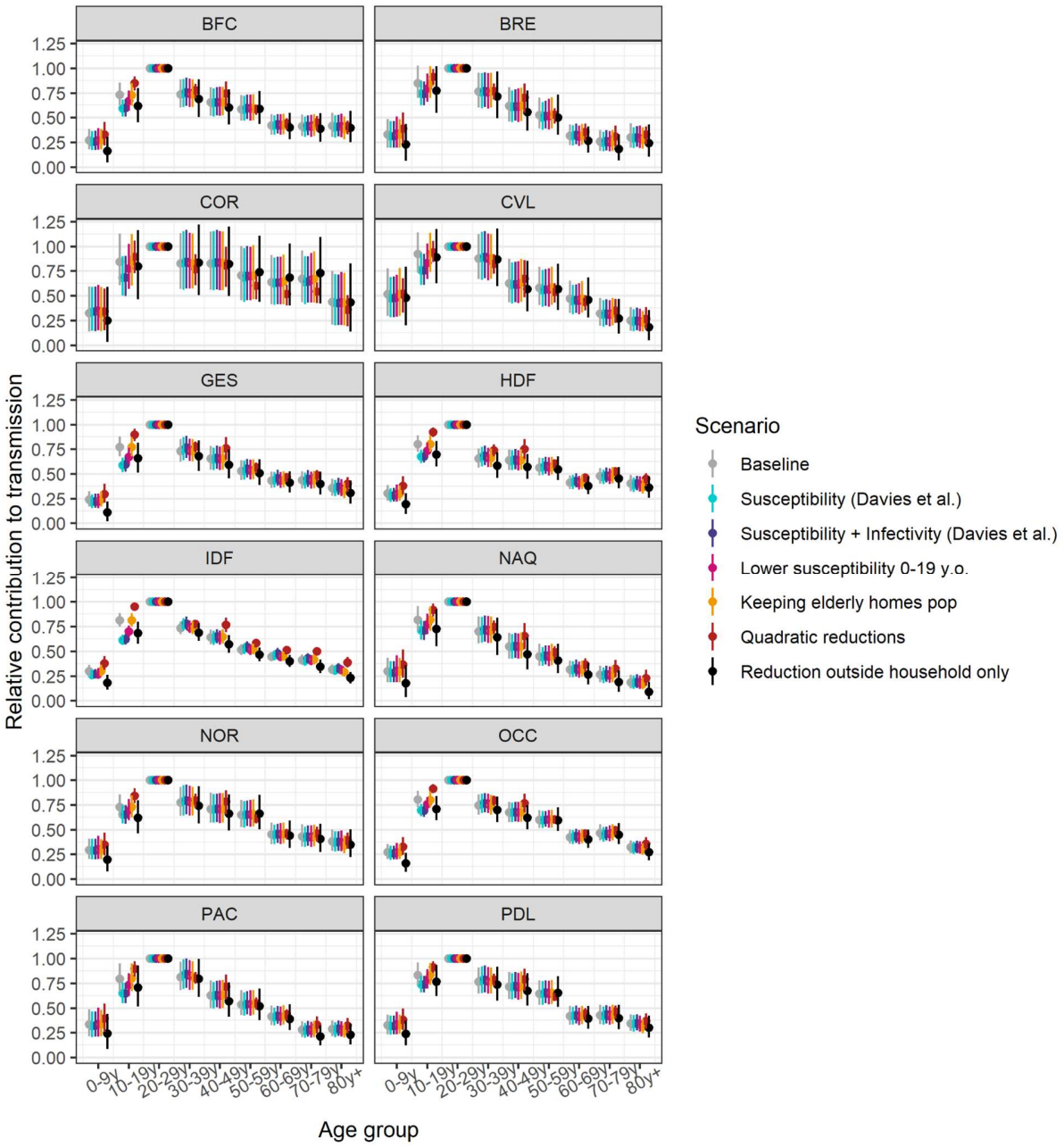

Figure S27: Sensitivity analyses - Relative contribution to transmission of the different age groups in the different regions (except Auvergne-Rhône-Alpes). Different scenarios are explored: The scenarios explored are: *Susceptibility (Davies et al.)* - Using age-specific susceptibilities [21] ; *Susceptibility + Infectivity (Davies et al.)* - Using age-specific susceptibilities and infectivities [21]; *Lower susceptibility 0-19 y.o.* - 0-9 y.o. and 10-19 y.o. are respectively 50% and 25% less susceptible to SARS-CoV-2 infection than 20 y.o. and older ; *Keeping elderly homes pop* - Including the population of elderly homes in the study population ; *Quadratic reduction* - Considering quadratic reductions in contact patterns ; *Reduction outside household only* - Assuming contact patterns are only modified outside the household.

Figure S28

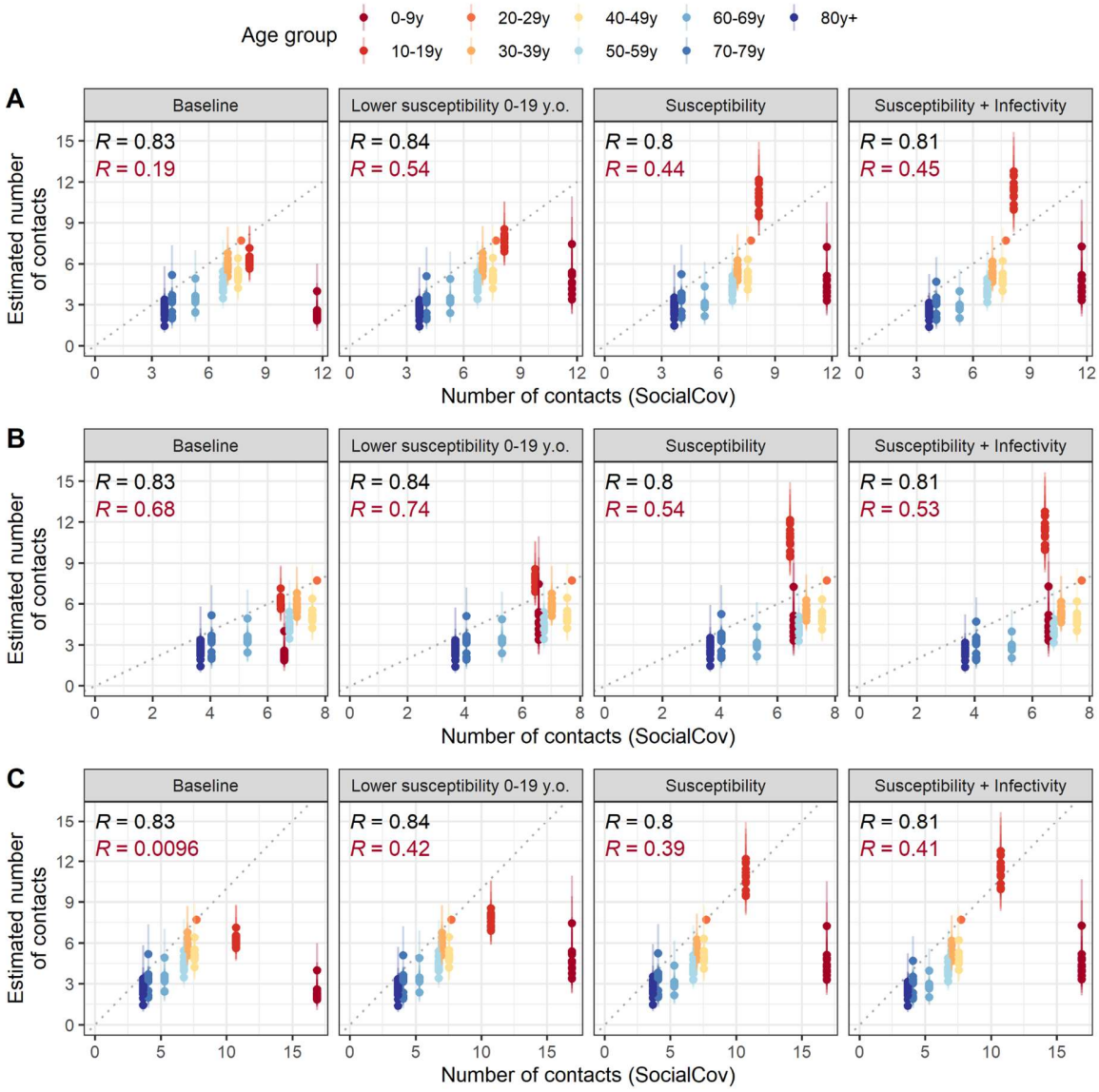

Figure S28: Comparison between the estimated number of contacts and the number of contacts measured in the SocialCov survey. (A) Using the contact survey data for 0-19 y.o. between July 30th, 2020 and September 27th, 2020. **(B)** Using the contact survey data for 0-19 y.o. between July 30th, 2020 and September 1st, 2020. **(C)** Using the contact survey data for 0-19 y.o. between September 1st, 2020 and September 27th, 2020. Different scenarios are explored: *Susceptibility* - Using age-specific susceptibilities [21]; *Susceptibility + Infectivity* - Using age-specific susceptibilities and infectivities [21]; *Lower susceptibility 0-19 y.o.* - 0-9 y.o. and 10-19 y.o. are respectively 50% and 25% less susceptible to SARS-CoV-2 infection than 20 y.o. and older. Each point (with linerange) corresponds to the estimate for a given region with 95% credible interval. The upper values of R (black) correspond to the Pearson's correlation coefficient removing the 0-9 y.o. and 10-19 y.o. age groups. The lower values of R (red) correspond to the Pearson's correlation coefficient using the data from all age groups.

Figure S29

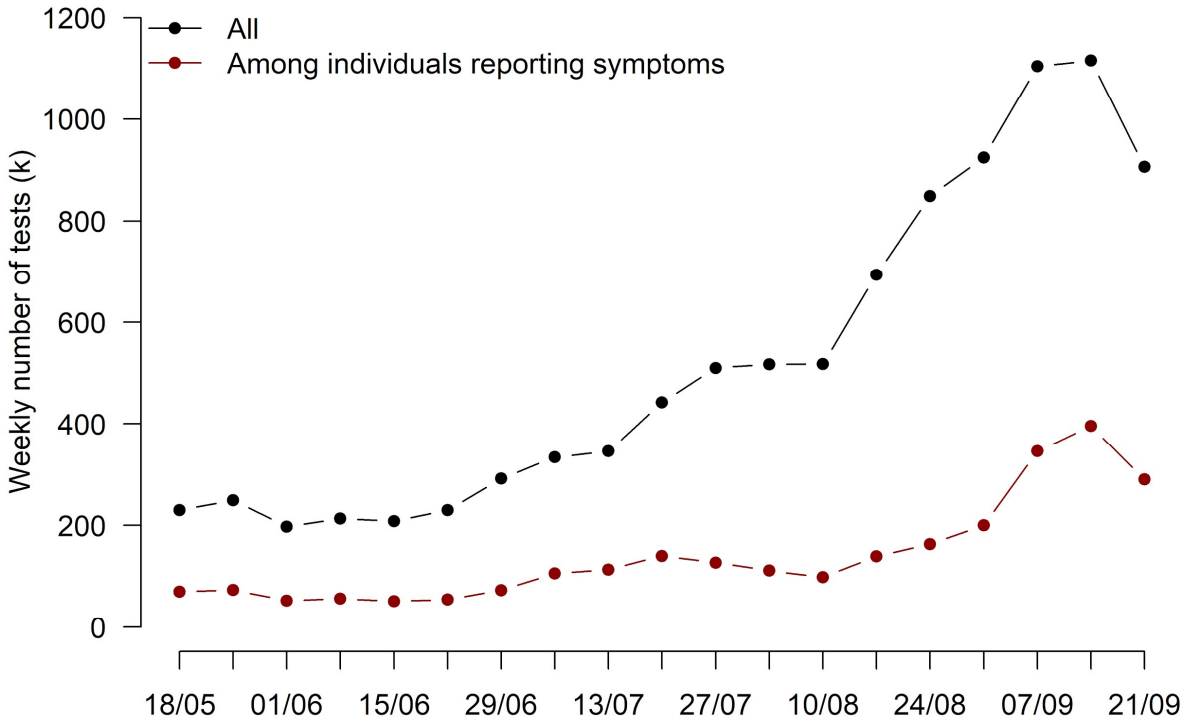

Figure S29: Number of tests performed per week reported in the SIDEP surveillance system in metropolitan France.

Figure S30

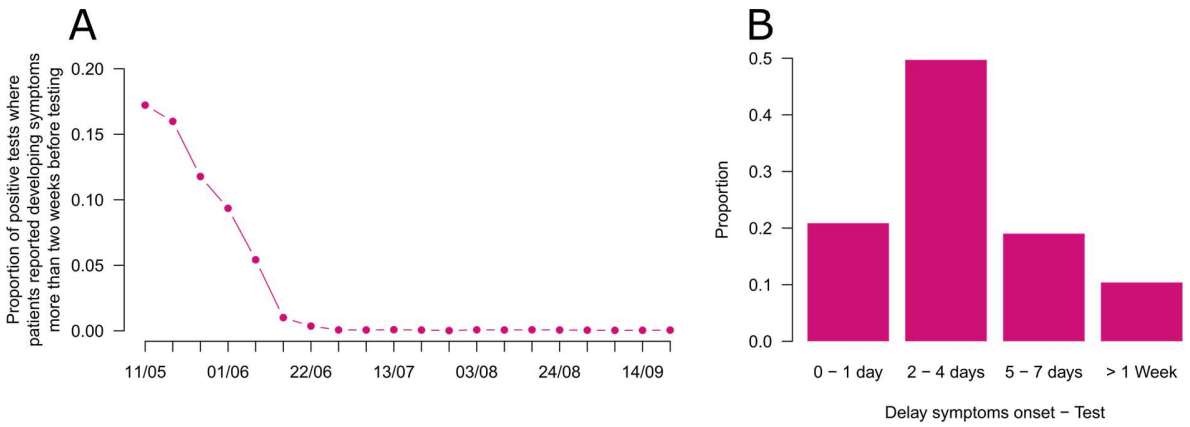

Figure S30: Characteristics of the delay between onset of symptoms and test. (A) Proportion of positive tests in patients reporting a delay greater than two weeks between symptoms onset more and testing by week of nasopharyngeal swab. **(B)** Distribution of the delay between symptoms onset and test for the time period 15 June 2020 - 27 September 2020.

Figure S31

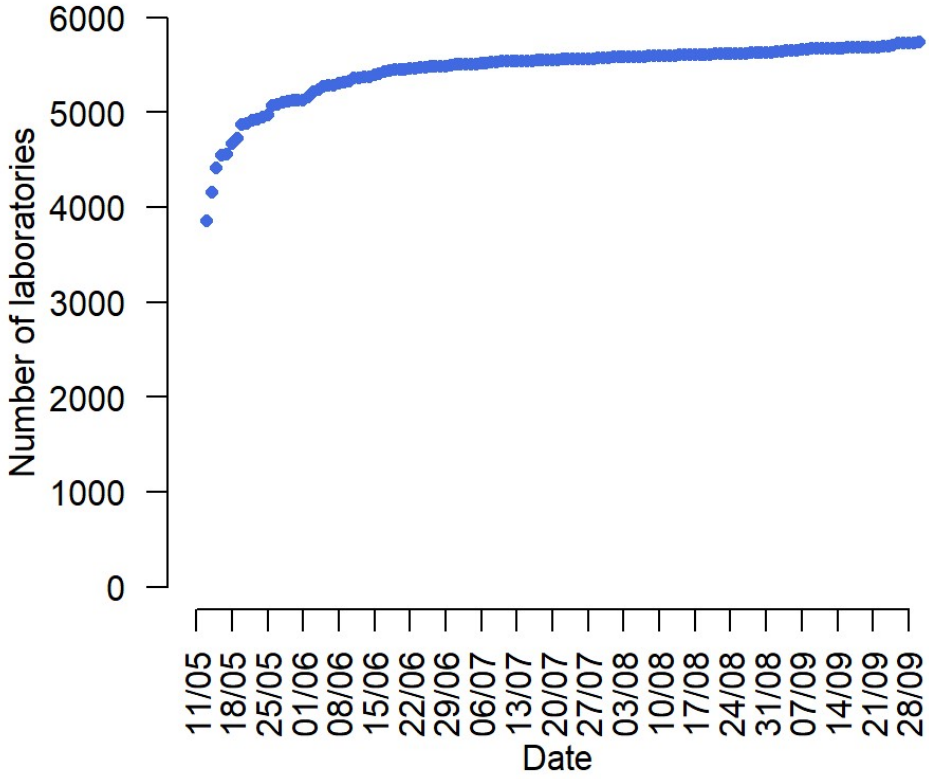

Figure S31: Number of laboratories reporting in the SIDEP database through time.

Table S1: Parameter 95% credible intervals

Parameters common to all the regions

Change in contact patterns during the post-lockdown period for individuals aged 0-9 y.o. $\alpha_{0-9y}{}^{postLock}$	0.51 (0.40 - 0.65)
Change in contact patterns during the post-lockdown period for individuals aged 10-19 y.o.$\alpha_{10-19y}{}^{postLock}$	1.13 (0.90 - 1.37)
Change in contact patterns during the post-lockdown period for individuals aged 30-39 y.o.$\alpha_{30-39y}{}^{postLock}$	0.81 (0.62 - 1.07)
Change in contact patterns during the post-lockdown period for individuals aged 40-49 y.o.$\alpha_{40-49y}{}^{postLock}$	0.51 (0.41 - 0.62)
Change in contact patterns during the post-lockdown period for individuals aged 50-59 y.o.$\alpha_{50-59y}{}^{postLock}$	0.62 (0.48 - 0.79)
Change in contact patterns during the post-lockdown period for individuals aged 60-69 y.o.$\alpha_{60-69y}{}^{postLock}$	0.58 (0.46 - 0.71)
Change in contact patterns during the post-lockdown period for individuals aged 70-79 y.o.$\alpha_{70-79y}{}^{postLock}$	0.64 (0.51 - 0.80)
Change in contact patterns during the post-lockdown period for individuals aged ≥80 y.o.$\alpha_{80y+}{}^{postLock}$	0.77 (0.60 - 1.01)
Prevalence of non-COVID infections with COVID suggestive symptoms in the population π	0.0060 (0.0058 - 0.0063)
Overdispersion parameter associated with the contribution to the likelihood of age-stratified hospitalization data δ_2	0.64 (0.58 - 0.69)
Overdispersion parameter associated with the contribution to the likelihood of age-stratified test data δ_3	0.46 (0.44 - 0.49)

Region-specific transmission parameters

Region	Post-lockdown reproduction number $R_{postLock}$	Epidemic rebound reproduction number $R_{rebound}$
ARA	0.90 (0.88 - 0.93)	1.46 (1.44 - 1.49)
BFC	0.96 (0.93 - 0.99)	1.50 (1.46 - 1.55)
BRE	0.89 (0.86 - 0.93)	1.31 (1.25 - 1.36)

COR	1.03 (0.99 - 1.06)	1.40 (1.31 - 1.50)
CVL	0.86 (0.83 - 0.90)	1.54 (1.46 - 1.62)
GES	1.05 (1.02 - 1.08)	1.46 (1.43 - 1.49)
HDF	0.97 (0.95 - 1.00)	1.39 (1.36 - 1.42)
IDF	1.11 (1.08 - 1.15)	1.58 (1.56 - 1.60)
NAQ	0.90 (0.88 - 0.93)	1.72 (1.65 - 1.80)
NOR	0.91 (0.88 - 0.94)	1.40 (1.37 - 1.44)
OCC	0.96 (0.94 - 0.99)	1.38 (1.35 - 1.40)
PAC	0.96 (0.93 - 0.99)	1.81 (1.73 - 1.88)
PDL	0.98 (0.95 - 1.01)	1.20 (1.17 - 1.22)

Region-specific contact parameters $\alpha_{Age}{}^{rebound}$

	Age-group								
Region	0-9y	10-19y	20-29y	30-39y	40-49y	50-59y	60-69y	70-79y	80y+
ARA	0.30 (0.23 - 0.39)	0.61 (0.52 - 0.72)	1 (ref)	0.80 (0.62 - 1.04)	0.55 (0.46 - 0.67)	0.91 (0.63 - 1.39)	0.69 (0.54 - 0.89)	0.66 (0.52 - 0.85)	0.62 (0.50 - 0.80)
BFC	0.32 (0.21 - 0.47)	0.62 (0.48 - 0.78)	1 (ref)	0.80 (0.55 - 1.17)	0.56 (0.42 - 0.76)	1.01 (0.58 - 1.82)	0.77 (0.52 - 1.23)	0.67 (0.46 - 1.01)	0.91 (0.52 - 1.90)
BRE	0.39 (0.23 - 0.62)	0.74 (0.53 - 1.01)	1 (ref)	0.92 (0.54 - 1.51)	0.54 (0.36 - 0.79)	0.88 (0.46 - 1.81)	0.54 (0.34 - 0.85)	0.38 (0.23 - 0.60)	0.58 (0.32 - 1.26)
COR	0.44 (0.18 - 0.84)	0.78 (0.50 - 1.13)	1 (ref)	1.07 (0.59 - 1.82)	0.87 (0.51 - 1.42)	1.46 (0.63 - 3.12)	1.56 (0.74 - 2.99)	1.57 (0.77 - 2.91)	1.08 (0.39 - 3.07)
CVL	0.73	0.88	1 (ref)	1.17	0.58	1.08	1.04	0.54	0.48

	(0.38 - 1.30)	(0.61 - 1.20)		(0.66 - 1.97)	(0.37 - 0.89)	(0.52 - 2.22)	(0.56 - 1.94)	(0.30 - 0.88)	(0.26 - 0.80)
GES	0.27 (0.19 - 0.37)	0.61 (0.50 - 0.76)	1 (ref)	0.79 (0.57 - 1.12)	0.53 (0.42 - 0.68)	0.76 (0.51 - 1.23)	0.75 (0.54 - 1.11)	0.64 (0.47 - 0.90)	0.58 (0.42 - 0.85)
HDF	0.34 (0.25 - 0.44)	0.63 (0.53 - 0.76)	1 (ref)	0.64 (0.49 - 0.84)	0.50 (0.40 - 0.61)	0.80 (0.54 - 1.27)	0.63 (0.48 - 0.85)	0.71 (0.52 - 0.99)	0.61 (0.47 - 0.89)
IDF	0.33 (0.27 - 0.40)	0.61 (0.52 - 0.70)	1 (ref)	0.84 (0.68 - 1.03)	0.50 (0.43 - 0.58)	0.61 (0.50 - 0.75)	0.61 (0.51 - 0.73)	0.51 (0.43 - 0.61)	0.42 (0.36 - 0.50)
NAQ	0.32 (0.20 - 0.50)	0.67 (0.52 - 0.87)	1 (ref)	0.78 (0.51 - 1.21)	0.44 (0.32 - 0.59)	0.65 (0.40 - 1.15)	0.52 (0.34 - 0.79)	0.38 (0.25 - 0.56)	0.30 (0.19 - 0.45)
NOR	0.37 (0.25 - 0.52)	0.63 (0.49 - 0.79)	1 (ref)	0.88 (0.61 - 1.28)	0.63 (0.47 - 0.85)	1.28 (0.69 - 2.19)	0.86 (0.58 - 1.34)	0.70 (0.48 - 1.02)	0.70 (0.48 - 1.15)
OCC	0.32 (0.23 - 0.43)	0.67 (0.57 - 0.80)	1 (ref)	0.80 (0.62 - 1.07)	0.57 (0.47 - 0.70)	1.01 (0.67 - 1.58)	0.72 (0.56 - 0.96)	0.78 (0.58 - 1.10)	0.56 (0.44 - 0.71)
PAC	0.41 (0.25 - 0.62)	0.68 (0.51 - 0.89)	1 (ref)	1.05 (0.69 - 1.56)	0.55 (0.40 - 0.74)	0.86 (0.53 - 1.52)	0.77 (0.51 - 1.19)	0.43 (0.30 - 0.60)	0.52 (0.36 - 0.74)
PDL	0.41 (0.29 - 0.56)	0.75 (0.60 - 0.93)	1 (ref)	0.90 (0.63 - 1.29)	0.65 (0.50 - 0.85)	1.24 (0.70 - 2.07)	0.73 (0.53 - 1.06)	0.69 (0.49 - 0.99)	0.62 (0.45 - 0.85)

Table S2: Mean daily number of contacts reported by participants of the SocialCov survey between 30 July 2020 and 27 September 2020.

Age group	**Mean daily number of contacts**	**95% bootstrap interval** (computed from 10,000 bootstrap samples)
0-9 y.o.	11.7	(10.0 - 13.5)
10-19 y.o.	8.1	(6.9 - 9.5)
20-29 y.o.	7.7	(6.9 - 8.7)
30-39 y.o.	7.0	(6.1 - 7.8)
40-49 y.o.	7.5	(6.8 - 8.4)
50-59 y.o.	6.7	(5.9 - 7.7)
60-69 y.o.	5.3	(4.4 - 6.4)
70-79 y.o.	4.1	(3.1 - 5.3)
≥80 y.o.	3.7	(1.3 - 6.4)

Table S3: Dates used for a change in transmission levels in regions in Metropolitan France.

Region	Date
Auvergne-Rhône-Alpes	09/07/2020
Bourgogne-Franche-Comté	23/07/2020
Bretagne	06/07/2020
Centre-Val de Loire	09/07/2020
Corse	06/08/2020
Grand Est	09/07/2020
Hauts-de-France	09/07/2020
Île-de-France	25/06/2020
Nouvelle-Aquitaine	23/07/2020
Normandie	17/07/2020
Occitanie	17/07/2020
Provence Alpes Côte d'Azur	17/07/2020
Pays de la Loire	03/07/2020

Table S4: Time windows used to calibrate the model in the different regions

Region	Time window
Auvergne-Rhône-Alpes	11/05/2020 - 27/09/2020
Bourgogne-Franche-Comté	11/05/2020 - 27/09/2020
Bretagne	11/05/2020 - 06/09/2020
Centre-Val de Loire	11/05/2020 - 31/08/2020
Corse	11/05/2020 - 27/09/2020
Grand Est	11/05/2020 - 27/09/2020
Hauts-de-France	11/05/2020 - 27/09/2020
Île-de-France	11/05/2020 - 27/09/2020
Nouvelle-Aquitaine	11/05/2020 - 06/09/2020
Normandie	11/05/2020 - 27/09/2020
Occitanie	11/05/2020 - 27/09/2020
Provence Alpes Côte d'Azur	11/05/2020 - 31/08/2020
Pays de la Loire	11/05/2020 - 27/09/2020

Table S5: Probabilities of ICU admission and death given hospitalization used in forward simulations. These estimates are computed based on hospital admissions reported in the SI-VIC surveillance system in September and October 2020. We use the central estimates in the forward simulations. 95% confidence intervals were computed from 1,000,000 bootstrap samples.

Age-group	Probability of ICU admission given hospitalization	Probability of death given hospitalization
0-19 y.o.	12.7% (10.7% - 14.8%)	0.2% (0.0% - 0.5%)
20-29 y.o.	11.0% (9.4% - 12.7%)	0.3% (0.1% - 0.6%)
30-39 y.o.	16.1% (14.6% - 17.6%)	1.1% (0.7% - 1.5%)
40-49 y.o.	20.8% (19.5% - 22.2%)	2.3% (1.8% - 2.7%)
50-59 y.o.	25.6% (24.4% - 26.7%)	4.5% (4.0% - 5.0%)
60-69 y.o.	32.1% (31.2% - 33.0%)	11.0% (10.4% - 11.6%)
70-79 y.o.	28.0% (27.2% - 28.8%)	18.6% (17.9% - 19.3%)
≥80 y.o.	8.5% (8.1% - 8.9%)	30.6% (30.0% - 31.1%)

Table S6: Percentage of hospital deaths arising among patients hospitalized in ICUs. These estimates are computed based on hospital admissions reported in the SI-VIC surveillance system in September and October 2020. We use the central estimates in the forward simulations (to compute quality adjusted life years). 95% confidence intervals were computed from 1,000,000 bootstrap samples.

Age-group	Proportion of deaths occuring in ICUs
0-19 y.o.	50% (0% - 100%)
20-29 y.o.	75% (25% - 100%)
30-39 y.o.	64% (44% - 84%)
40-49 y.o.	61% (51% - 71%)
50-59 y.o.	61% (55% - 66%)
60-69 y.o.	67% (64% - 70%)
70-79 y.o.	55% (52% - 57%)
≥80 y.o.	14% (13% - 15%)

Table S7: Weights used to compute the number of life years lost and the number of quality adjusted life years lost.

Age group	Weights for the computation of the number of life years lost	Weights for the computation of the number of quality adjusted life years lost
0-9 y.o.	78.4 years	66.6 years
10-19 y.o.	65.5 years	56.7 years
20-29 y.o.	58.7 years	47.2 years
30-39 y.o.	49.0 years	38.5 years
40-49 y.o.	39.4 years	30.3 years
50-59 y.o.	30.4 years	22.9 years
60-69 y.o.	22.1 years	16.2 years
70-79 y.o.	14.4 years	10.3 years
≥80 y.o.	6.9 years	4.9 years